



Rapid Initial Morphospace Expansion and Delayed Morphological Disparity Peak in the First 100 Million Years of the Archosauromorph Evolutionary Radiation

Christian Foth^{1,2*}, Roland B. Sookias^{3,4,5} and Martín D. Ezcurra^{6,7}

¹Department of Geosciences, University of Fribourg, Fribourg, Switzerland, ²State Museum of Natural History Stuttgart, Stuttgart, Germany, ³Evolution and Diversity Dynamics Lab, Department of Geology, University of Liège, Liège, Belgium, ⁴Department of Earth Sciences, University of Oxford, Oxford, United Kingdom, ⁵Museum für Naturkunde, Leibniz-Institut für Evolutions- und Biodiversitätsforschung, Berlin, Germany, ⁶Sección Paleontología de Vertebrados, CONICET–Museo Argentino de Ciencias Naturales “Bernardino Rivadavia”, Buenos Aires, Argentina, ⁷School of Geography, Earth and Environmental Sciences, University of Birmingham, Birmingham, United Kingdom

OPEN ACCESS

Edited by:

Fabien Knoll,
Fundacion Agencia Aragonesa para la
Investigacion y el Desarrollo, Spain

Reviewed by:

Pedro L. Godoy,
Federal University of Paraná, Brazil
Tom Stubbs,
University of Bristol, United Kingdom

*Correspondence:

Christian Foth
christian.foth@gmx.net

Specialty section:

This article was submitted to
Paleontology,
a section of the journal
Frontiers in Earth Science

Received: 11 June 2021

Accepted: 17 August 2021

Published: 07 September 2021

Citation:

Foth C, Sookias RB and Ezcurra MD
(2021) Rapid Initial Morphospace
Expansion and Delayed Morphological
Disparity Peak in the First 100 Million
Years of the Archosauromorph
Evolutionary Radiation.
Front. Earth Sci. 9:723973.
doi: 10.3389/feart.2021.723973

Adaptive radiations have played a major role in generating modern and deep-time biodiversity. The Triassic radiation of the Archosauromorpha was one of the most spectacular vertebrate radiations, giving rise to many highly ecomorphologically varied lineages—including the dinosaurs, pterosaurs, and stem-crocodylians—that dominated the larger-bodied land fauna for the following 150 Ma, and ultimately gave rise to today’s > 10,000 species of birds and crocodylians. This radiation provides an outstanding testbed for hypotheses relating to adaptive radiations more broadly. Recent studies have started to characterize the tempo and mode of the archosauromorph early adaptive radiation, indicating very high initial rates of evolution, non-competitive niche-filling processes, and previously unrecognized morphological disparity even among non-crown taxa. However, these analyses rested primarily either on discrete characters or on geometric morphometrics of the cranium only, or even failed to fully include phylogenetic information. Here we expand previous 2D geometric morphometric cranial datasets to include new taxa and reconstructions, and create an analogous dataset of the pelvis, thereby allowing comparison of anatomical regions and the transition from “sprawling” to “upright” posture to be examined. We estimated morphological disparity and evolutionary rates through time. All sampled clades showed a delayed disparity peak for sum of variances and average nearest neighbor distances in both the cranium and pelvis, with disparity likely not saturated by the end of the studied time span (Late Jurassic); this contrasts with smaller radiations, but lends weight to similar results for large, ecomorphologically-varied groups. We find lower variations in pelvic than cranial disparity among Triassic-Jurassic archosaurs, which may be related to greater morphofunctional constraints on the pelvis. Contrasting with some previous work, but also confirming some previous findings during adaptive radiations, we find relatively widespread evidence of correlation between sampled diversity and disparity, especially at the largest phylogenetic scales and using average displacement rather than sum of variances as

disparity metric; this also demonstrates the importance of comparing disparity metrics, and the importance of phylogenetic scale. Stem and crown archosauromorphs show a morphological diversification of both the cranium and pelvis with higher initial rates (Permian–Middle Triassic and at the base of major clades) followed by lower rates once diversification into niches has occurred (Late Triassic–Jurassic), indicating an “early burst” pattern *sensu lato*. Our results provide a more detailed and comprehensive picture of the early archosauromorph radiation and have significant bearing on the understanding of deep-time adaptive radiations more broadly, indicating widespread patterns of delayed disparity peaks, initial correlation of diversity and disparity, and evolutionary early bursts.

Keywords: Archosauromorpha, Archosauria, geometric morphometrics, disparity, evolutionary rates, early Mesozoic, adaptive radiation

INTRODUCTION

Evolutionary radiations—instances of unusually rapid phylogenetic diversification, often triggered by colonization of new habitats, extinction events freeing niche space, or key innovations (Simões et al., 2016)—have been central in the generation of modern and deep-time biodiversity, and have long been a major focus of evolutionary research. These events are often associated with exceptional levels of morphological diversification into new habitats and ecological niches, and are termed adaptive radiations (Schluter, 2000; Wesley-Hunt, 2005). At geological scales, adaptive radiations have given rise to many of the most spectacular and successful groups of animals and plants on Earth, including the flowering plants (Heimhofer et al., 2005), beetles (Bernhardt, 2000), birds (Cooney et al., 2017), and placental mammals (Madsen et al., 2001). At smaller temporal scales (sometimes considered adaptive radiations *sensu stricto*—Schluter 2000), they have given rise to groups of highly varied but closely related taxa exquisitely adapted to particular niches (Pinto et al., 2008; Abzhanov 2010), with the adaptive radiation of *Geospiza* finches having famously aided Darwin in formulating the theory of evolution by natural selection (Abzhanov 2010). Studying the dynamics of these events allows us to better understand the process of evolution and the generation of biodiversity itself, addressing questions such as how long after an adaptive radiation morphological diversity (i.e., disparity) tends to become saturated (Hughes et al., 2013), the correlation of morphological disparity with taxic diversity (Ruta et al., 2013; Puttick et al., 2020), whether elevated rates of evolution occur and how long they last (Puttick, 2018; Hernández-Hernández, 2019), the relative importance of competitive- and non-competitive processes in diversification (Brusatte et al., 2008a; Benson et al., 2014), and the underlying reasons for the success and radiation of particular lineages (Seehausen, 2006; Jønsson et al., 2012).

The initial radiation of Archosauria and their stem lineage represents one of the most important geologic-scale vertebrate adaptive radiations in Earth history (Ezcurra and Butler, 2018; Ezcurra et al., 2021a), and provides an outstanding testbed for answering major questions relating to adaptive radiation more

broadly. Archosaurs originated approximately 248 Ma ago (late Olenekian; Butler et al., 2011), with the clade thus having a very long evolutionary history and persisting until today as an extraordinarily successful group represented by birds and crocodylians. Extant archosaurs are represented by c. 10,000 species of birds (Jetz et al., 2012), varying in their morphology from the ~3 m tall (140 kg) flightless ostrich *Struthio camelus* to the tiny (2 g) nectarivore, hovering, bee hummingbird *Mellisuga helenae* (Bird Life International, 2020). By contrast, although crocodylians are far less speciose (c. 24 species) and morphologically disparate than birds, they are geographically widespread and inhabit both freshwater and marine environments of equatorial and subtropical latitudes (Grenard, 1991). Archosaurs and their closest relatives have been the most diverse and abundant medium to large-sized vertebrate components of terrestrial assemblages for more than 150 Ma during most of the Mesozoic, and occupied most of the ecological niches exploited by mammals in Cenozoic ecosystems (Brusatte et al., 2008a; Sookias et al., 2012; Benton et al., 2014). Both bird- (Aves) and crocodile-line (Pseudosuchia) archosaurs were extraordinarily morphologically diverse during the Mesozoic; avemetatarsalians ranged from the tiny fish-eating first pterosaurs (Bestwick et al., 2018) to the largest land animals in Earth history—the sauropod dinosaurs (Sander et al., 2011)—, while pseudosuchians included herbivorous (e.g. Wu et al., 1995; Kley et al., 2010; Desojo et al., 2013), hypercarnivorous species (e.g. Nesbitt et al., 2013), and continental, freshwater and marine forms (e.g. Li et al., 2006; Ósi et al., 2018; Butler et al., 2019a). Given their key importance in both modern and ancient ecosystems, and immense ecomorphological variety, understanding the origin and evolutionary radiation of Archosauria is of major scientific interest.

Archosauromorpha (= archosaurs and their stem lineage) diversified following the end-Permian mass extinction (Ezcurra, 2016; Ezcurra and Butler, 2018; Ezcurra et al., 2021b), the most severe biotic crisis documented in the history of life (Raup and Sepkoski, 1982; Benton, 2003). As a result of this extinction, the previously diverse non-mammalian synapsids crashed in abundance and morphological diversity, freeing ecospace into which archosauromorphs radiated (Sookias et al., 2012). This first evolutionary radiation of

archosauromorphs included many stem-archosaurs with an extremely diverse ecology and morphology (Ezcurra et al., 2021a), including specialized herbivores (Nesbitt et al., 2015; Ezcurra et al., 2016), hypercarnivores (Gower, 2003; Butler et al., 2019b), ground-dwelling smaller predators (Sookias et al., 2020), marine (Jaquier et al., 2017; Spiekman and Scheyer, 2019), and probably even gliding species (Sharov, 1971; Dzik and Sulej, 2016). They formed important components of Triassic ecosystems (Foth et al., 2016a), but have tended to be overlooked due to a focus on the origins and radiation of crown archosaur groups (e.g. dinosaurs, pterosaurs and pseudosuchians) (Ezcurra et al., 2021b).

Recently, the importance of stem-archosaurs has begun to be understood. Non-crown taxa have been found to be unexpectedly morphologically diverse, with skeletal (based on discrete characters) and lineage diversification being especially high immediately following the end-Permian mass extinction event (Ezcurra and Butler 2018; Ezcurra et al., 2021a), and cranial disparity (based on 2D geometric morphometric data) at least as high if not higher than contemporaneous crown archosaurs (Foth et al., 2016a). Indeed, the extinction of many of these non-crown taxa between the Middle and Late Triassic may have allowed, at least in part, crown archosaurs—including early dinosaurs—to diversify as spectacularly as they did (Foth et al., 2016a).

These recent findings rest, however, primarily on analyses of discrete character changes or cranial shape only (Foth et al., 2016a; Ezcurra and Butler, 2018; Ezcurra et al., 2021a). Discrete characters are widely used in disparity analyses to study complete body plans, but they are not as powerful as geometric morphometric methods to capture anatomical variation (Anderson and Friedman, 2012). The analysis of cranial shape has been conducted using geometric morphometrics and certainly corresponds to some extent to ecomorphological diversity (Verde Arregoitia et al., 2017; Michaud et al., 2018), but it is by no means a comprehensive proxy for ecomorphological evolution (Michaud et al., 2018; Navalón et al., 2018). Locomotor morphology also undoubtedly played a role in dictating ecological niche (Higham and Russell, 2010; Jorgensen and Reilly, 2013). Furthermore, locomotor morphology continues to be the subject of much discussion in the context of Triassic archosauromorph evolution in particular, because one of the apparent key transitions witnessed in this lineage is that from a sprawling gait, similar to that of many extant lizards, to an upright locomotor mode typical of most dinosaurs (including birds) and some crocodile-line taxa (Hutchinson, 2001; Hutchinson, 2006).

Previous geometric morphometric-based disparity analyses have also failed to take phylogenetic knowledge fully into account, which can have a major impact on our understanding of evolutionary patterns (Cavin and Forey, 2007). Although some former work did include hypothetical ancestral taxa (Brusatte et al., 2011; Foth et al., 2016a), it did not account for the so called ghost and Lazarus lineages (lineages not recorded but inferred to be present due to the presence of their sister taxa in a time interval and of the lineage itself in a later time interval, and lineages inferred to be present due to their presence either side of an interval but not recorded in that

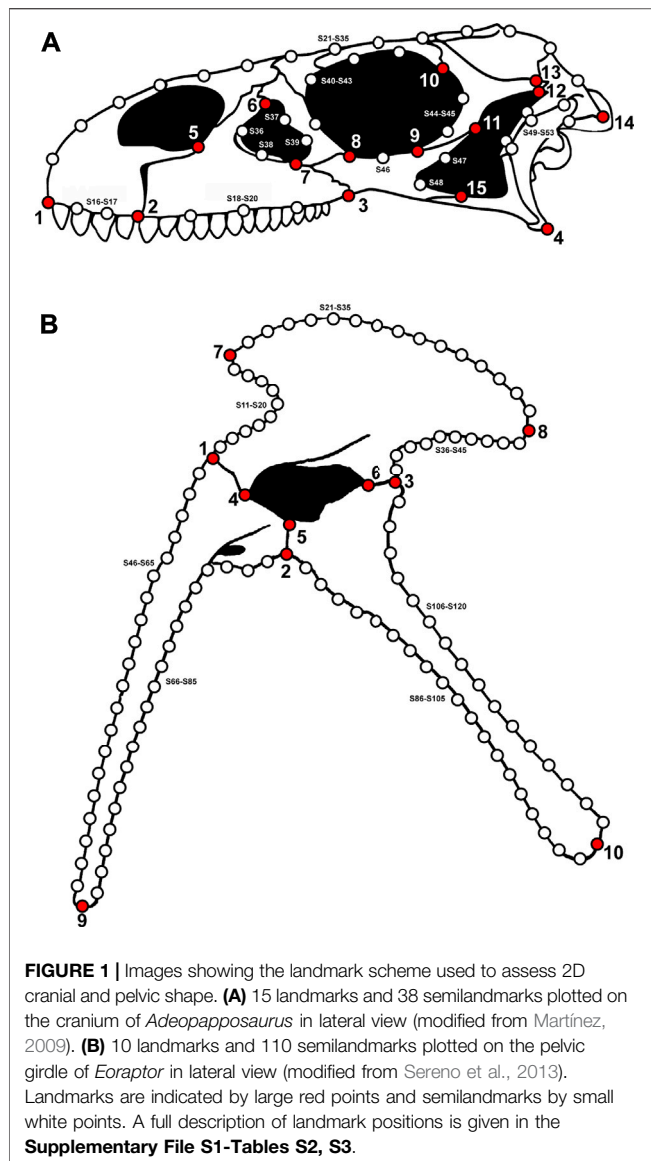
interval, respectively), which—given the relatively low overall taxon sampling during the early archosaur radiation—is likely to have a major impact on the results. Furthermore, previous geometric morphometric-based studies did not examine rates of evolutionary change, rather taking only a bin-based time series approach. Elevated rates of evolution and subsequent slowdown as niche space is filled have been considered to be central to adaptive radiations (Close et al., 2015; Clarke et al., 2017) and were previously found for archosauromorphs on the basis of discrete characters (Ezcurra and Butler, 2018; Ezcurra et al., 2021a). Thus, examining whether similar patterns are found in the archosauromorph radiation using geometric morphometric data promises to broaden our understanding of both this radiation and evolutionary processes.

Here, we aim to improve our understanding of late Permian to Late Jurassic archosauromorph morphological evolution by incorporating new cranial reconstructions additional to those used in previous studies (Foth et al., 2016a), expanding the analysis to the locomotor region (pelvic shape), and fully incorporating phylogenetic knowledge (ghost and Lazarus lineages). We compare cranial and pelvic disparity against one another and between groups and time intervals, focusing on the comparison between stem- and crown-archosaurs. We also examine the interaction of diversity and disparity. Furthermore, we directly test rates of evolution with a recently developed multivariate approach, using both cranial and pelvic landmark datasets, to examine whether rates were especially elevated around the base of the archosauromorph radiation and/or in certain, more deeply nested groups, and whether rates were higher in crown than in stem-archosaurs or vice versa. Overall, we aim to provide a more detailed and comprehensive picture of the early adaptive radiation of stem and crown archosaurs that may help to elucidate the reasons for their success, and shed light on the process of adaptive radiation over geological timescales more broadly.

MATERIALS AND METHODS

Taxon Sampling and Geometric Morphometrics

We updated the dataset of two-dimensional landmarked images of archosauromorph crania (excluding the mandible) used by Foth et al. (2016a). Fifteen new archosauromorph species were added, the non-saurian diapsid *Youngina capensis* was included as the outgroup taxon, and two reconstructions were replaced with updated versions (*Euparkeria capensis* and *Rhynchosaurus articeps*). We sampled only non-monofenestratan pterosaurs, because our landmark scheme is not applicable to the merged external naris and antorbital fenestra of monofenestratan taxa. The updated cranial dataset includes 108 archosauromorph species, spanning from the late Permian to the Late Jurassic. In addition, we built a second dataset to explore shape variation of archosauromorph hemipelves. This dataset contains 73 archosauromorph species and *Youngina capensis* as the outgroup taxon. All landmarked images were based on published illustrations or reconstructions of adult (or advanced



subadult) individuals in lateral view (see **Supplementary File S1-Table S1**). All samples were carefully evaluated in terms of completeness and degree of taphonomic damage and deformation of the original fossil material (based on photographs or first-hand observations) in order to minimize the impact of these factors on shape analyses (Foth and Rauhut, 2013). Reconstructions relying on very incomplete or strongly deformed material were excluded.

We used two-dimensional geometric morphometrics to investigate variation in cranial and pelvic morphology. Cranial shape in lateral view was captured with 15 landmarks and 38 semilandmarks (see Foth et al., 2016a), while pelvic shape in lateral view was described by 10 landmarks and 110 semilandmarks (**Figure 1**; **Supplementary File S1-Tables S2, S3**). The landmarks used in this study were classified as either type 1 (defined along the articulation between two elements) or type 2 (points of maximum curvature and extremities)

(Bookstein, 1991). Cranial openings and overall outline shape of crania and pelves were captured by semilandmarks, which were plotted at equidistant intervals along the curves of the structures they were defining (Bookstein, 1991; Bookstein et al., 1999). All landmarks and semilandmarks were plotted with the software *tpsDig2* (Rohlf, 2005). The primary data were loaded into *MorphoJ* (Klingenberg, 2011) and superimposed using Generalized Procrustes Analysis (GPA) (Rohlf and Slice, 1990), which reduces variation between specimens caused by scale, translation (i.e. position) and rotation, leaving only shape variation (**Supplementary Files S2, S3**). Although semilandmarks contain less shape information due to their dependence on the position of other landmarks (Bookstein, 1997; Gunz et al., 2004; Zelditch et al., 2012), we treated landmarks and semilandmarks as equivalent for GPA (Zelditch et al., 2012) because in some aberrant species the sliding process can create considerable artificial deformation of the Procrustes shape (i.e. the shape after GPA; Foth et al., 2016b). The Procrustes coordinates were then converted into a covariance matrix and subjected to a reduction of dimensionality via a Principal Components Analysis (PCA), also in *MorphoJ* (**Supplementary Files S2, S3**). This method transforms the variation among individuals into new sets of independent variables (principal components) that are linear combinations, with zero covariance, of the original set. The resulting principal components (PCs) describe successively smaller amounts of total variation so that a large proportion of variation can be described by a small number of variables (Hammer and Harper, 2006; Zelditch et al., 2012). Thus, they define a morphospace that depicts the overall spread of variation among taxa in a relatively low number of dimensions, and can be used as proxies in macroevolutionary analyses to quantify major trends in shape evolution.

Disparity Analyses, Phylogeny, and Time Calibration

In the study of Foth et al. (2016a), PC scores of hypothetical ancestors were added to increase the sampling of the disparity analysis, partially filling gaps in the fossil record where archosauromorphs are poorly sampled but must have been more diverse based on phylogenetic ghost lineages (Brusatte et al., 2011). Wilberg (2017) presented an updated method based on the work of Friedman (2009) that fully embraces phylogenetic data by interpolating traits between nodes along the branches of the tree. This protocol is more efficient in minimizing the effects of artefacts related to sampling gaps in the fossil record (Foth et al., 2017) and it is employed here (see below).

We assembled an updated version of the informal supertree of Foth et al. (2016a) with a total of 206 species based on current phylogenetic hypotheses for archosauromorph clades, including all taxa from the cranial and pelvic datasets as well as 49 additional taxa for time calibration, which were later pruned (**Supplementary File S1-Table S1**; **Supplementary File S4**). The supertree was time-calibrated using the *bin_timePaleoPhy* function of the package *paleotree v.2.7* (Bapst, 2012) in *R*

v.3.5.1 (R Development Core Team, 2011), based on chronostratigraphic ranges (biochron or temporal uncertainty) of terminal taxa taken from the Paleobiology Database (www.paleobiodb.org) and recent literature (**Supplementary File S1-Table S1**). In order to take into account uncertainties introduced by inaccuracies associated with the age of fossils, we produced a set of 1,000 trees in which the polytomies of the supertree were resolved randomly prior to time-scaling, and the ages of the fossil observations were drawn randomly from a uniform distribution spanning the duration of the stratigraphic unit in which the fossils were found. All nodes were scaled by evenly distributing the available time between branches (the “equal” time-scaling method implemented in *bin_timePaleoPhy*, with the “vartime” parameter set to 1 million years) (Brusatte et al., 2008b). The recovered average of the root times is of 255.9 Ma.

In order to analyse disparity through time, taxa were binned into approximately equal time intervals spanning the late Permian to Tithonian (Late Jurassic). Taxa from the Wuchiapingian and Changhsingian (late Permian), Induan and Olenekian (Early Triassic), Aalenian and Bajocian (Middle Jurassic I), and Bathonian and Callovian (Middle Jurassic II) were combined into single bins, whereas the Norian was split in half into early and late Norian bins with their boundary at 217.8 Ma.

In the case of the cranium, the first seven PCs, which contain the most relevant shape information, were used for the disparity analyses, which were selected on the basis of the broken-stick method (de Vita, 1979; Jackson, 1993) performed in *PAST 3.05* (Hammer et al., 2001). For pelvic disparity, four PCs were taken into account after following the latter method. The PC values were mapped onto the set of time-calibrated supertrees using the *anc.recon* function of the *R* package *Rphylopars v.0.2.9* (Goolsby et al., 2017), which computes maximum-likelihood (ML) estimates of nodal trait values assuming a Brownian motion model with a constant rate of diffusion. Because of the generally poor fossil record of pseudosuchians in the Jurassic (Bronzati et al., 2015), we added 14 additional pseudosuchian species from younger time intervals (Early Cretaceous–Late Cretaceous) to the supertree and morphometric dataset, allowing reconstruction of more reliable ancestral shapes for those branches with a Jurassic origin (see Foth et al., 2016a).

Using a linear interpolation on the time-scaled tree branches [“gradual model” of Friedman (2009)], the PC values observed and reconstructed at the nodes of the trees were then used to compute the PCs along the branches of the trees, in particular at the midpoint of each time bin crossed by a particular branch (Friedman, 2009; Foth et al., 2017; Wilberg, 2017). Because the phylogeny is characterized by many long ghost lineages, the ‘punctuated’ model was not applied, as it would imply unrealistic conservation of morphologies during very long time periods for the archosauromorph cranial and hip evolution.

Temporal disparity patterns were estimated for all archosauromorphs, non-archosaurian archosauromorphs, crown archosaurs, and various archosaurian subclades, including pseudosuchians, avemetatarsalians, pterosaurs, dinosaurs, ornithischians, sauropodomorphs, and theropods. In addition, disparity was also explored for all archosauromorphs using the residuals of the regression

between eigenvalues and log-transformed centroid size to test the impact of removing allometric variation. A comprehensive assessment of a trait-space should include descriptions of its volume, density, and position, which are mathematically sampled by different space occupancy metrics (Guillerme et al., 2020). Therefore, we chose three different types of disparity metrics: 1) as volume metric we chose sum of variances, which measures the amount of the trait-space that is occupied by observations and is more robust to sample size than other metrics (e.g. sum of ranges; Wills, 2001; Guillerme et al., 2020); 2) average nearest neighbour distance was chosen as density metric, which measures the distribution of pairs of observations within a group in the trait-space (Foote, 1991; Guillerme et al., 2020); and 3) average displacements was chosen as a position metric that measures the ratio between the observations’ position (=average position of all samples per bin) relative to the centroid of the total trait space of each (sub-)clade investigated (the absence of displacement is represented by a value of 1, or 0 if the metric is log-transformed; Guillerme et al., 2020). For each group, all three disparity metrics were calculated using the branch interpolation PC values at the midpoint of the temporal duration of each bin. This was done using functions of the *R* package *disPRity v.1.4.1* (Guillerme, 2018). Using the results recovered from the 1,000 randomly resolved trees, we estimated the minimum, maximum and median curves of each metric, allowing assessment of the overall temporal patterns and their sensitivity to differences in topology and time-calibrations. Finally, we constructed confidence intervals using the 2.5 and 97.5% quantiles of each bin.

To test how the trends of disparity are driven by sample size, we compared the cranial and pelvic median disparity curves (for each clade and each disparity metric) against the number of observations per bin (hereafter sampled diversity) and the medians of the cranial and pelvic averaged rates through time using a generalized least-squares regression (GLS) with a first order autoregressive model (*corARMA*) using the function *gls* of the *R* package *nlme v.3.1-137* (Pinheiro et al., 2018). Average displacements were log-transformed before the regressions because of high differences between the maximum and minimum values. We calculated likelihood-ratio based pseudo- R^2 values using the function *r.squaredLR* of the *R* package *MuMIn v.1.40.4* (Bartoń, 2018). Finally, we tested if the cranial and pelvic disparities (of each clade and each metric) converge on a common signal through time using the same methods.

Evolutionary Rates

Evolutionary rate analyses were conducted with the *R* package *RRphylo v.2.0.6* (Castiglione et al., 2018). This uses the model free approach phylogenetic ridge regression to calculate rates of evolution in quantitative traits on phylogenies and automatically pinpoint evolutionary rate shifts, being applicable to multivariate datasets and non-ultrametric trees (Castiglione et al., 2018). The principal component axes accounting for c. 80% of the variance (first seven for cranium, four for pelvis, see above) were used as traits. Shift points and tip rates were identified using the *search.shift* function (with *auto.recognise* on). Trends and rates through time were

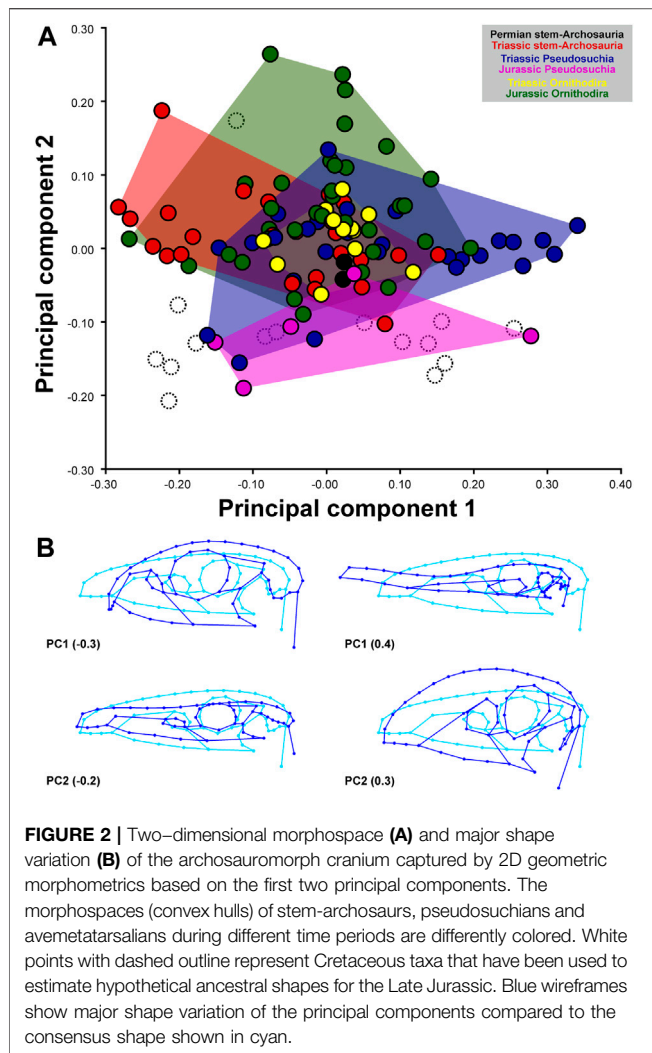


FIGURE 2 | Two-dimensional morphospace (A) and major shape variation (B) of the archosauromorph cranium captured by 2D geometric morphometrics based on the first two principal components. The morphospaces (convex hulls) of stem-archosaurs, pseudosuchians and avemetatarsalians during different time periods are differently colored. White points with dashed outline represent Cretaceous taxa that have been used to estimate hypothetical ancestral shapes for the Late Jurassic. Blue wireframes show major shape variation of the principal components compared to the consensus shape shown in cyan.

identified with the *search.trend* function (Castiglione et al., 2019). Analyses of the taxon sample as a whole were carried out in each of the 1,000 randomly resolved and time-calibrated (using range) trees for both cranial and pelvic datasets. These analyses were also conducted using residuals of the regression between eigenvalues and log-transformed centroid size to test the effect of removing allometric variation. Furthermore, analyses comparing clades bracketed by specific nodes to the rest of the tree were also conducted using the *search.trend* function. Each clade was compared to all other taxa in terms of estimated marginal means (EMM, i.e. the relative rate) and also the slope of change in rate through time. This was undertaken for the major clades Archosauria, Pseudosuchia, Dinosauria, Pterosauria, and the dinosaur groups Sauropodomorpha, Theropoda and Ornithischia. Rates through time were also examined as time series by binning rates on branches using the same time bins as used for the raw disparity data. Rates for branches were obtained from trend objects output by *RRphylo*, and were placed in all bins which the branch overlapped. End points for branches were taken from the trend object while start

points for branches were obtained using a custom function (“timeTREE” courtesy of Pasquale Raia—given in **Supplementary File S5**). The median rate was taken from the sample of rates across all trees and tested for correlation with time and between the skull and pelvis using generalized least squares regression in *R*, both with and without a first order autoregressive model. Regression without autocorrelation provides a rough test of a pattern of change in the data, but an autoregressive model provides a more robust test of a consistent trend throughout the series because successive time bins tend to show correlation with one another. Furthermore, a generalized random walk model with trend and an unbiased random walk model were fitted to the mean (and sample size, and variance) using the package *paleoTS* (Hunt, 2006) and their relative fits compared using AICc.

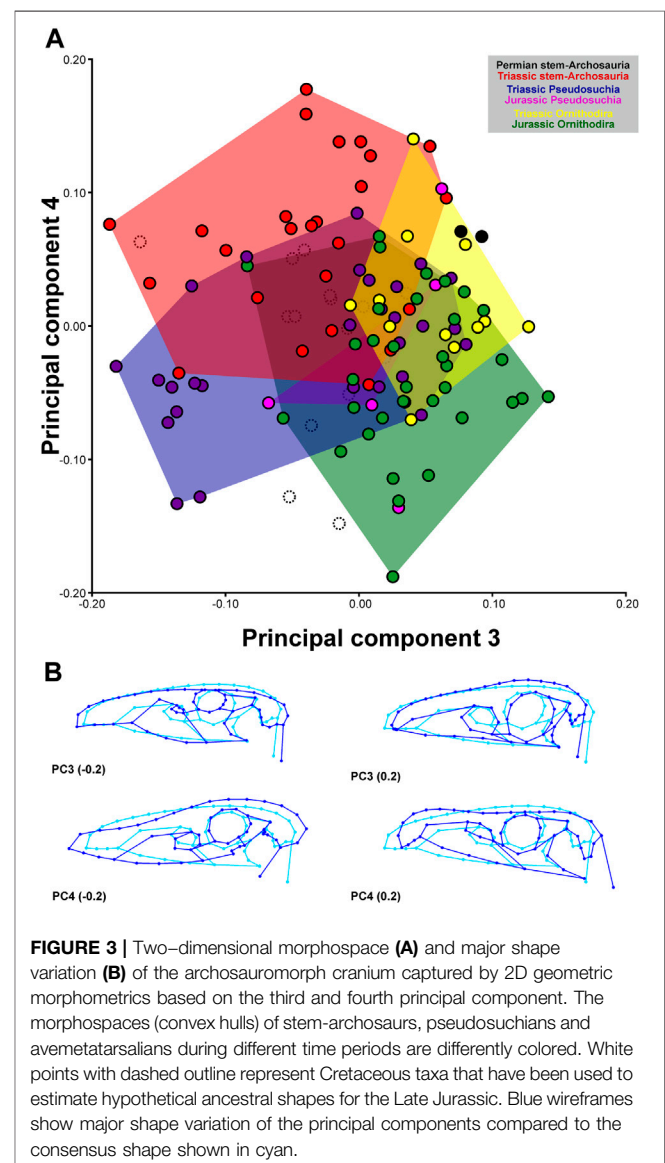


FIGURE 3 | Two-dimensional morphospace (A) and major shape variation (B) of the archosauromorph cranium captured by 2D geometric morphometrics based on the third and fourth principal component. The morphospaces (convex hulls) of stem-archosaurs, pseudosuchians and avemetatarsalians during different time periods are differently colored. White points with dashed outline represent Cretaceous taxa that have been used to estimate hypothetical ancestral shapes for the Late Jurassic. Blue wireframes show major shape variation of the principal components compared to the consensus shape shown in cyan.

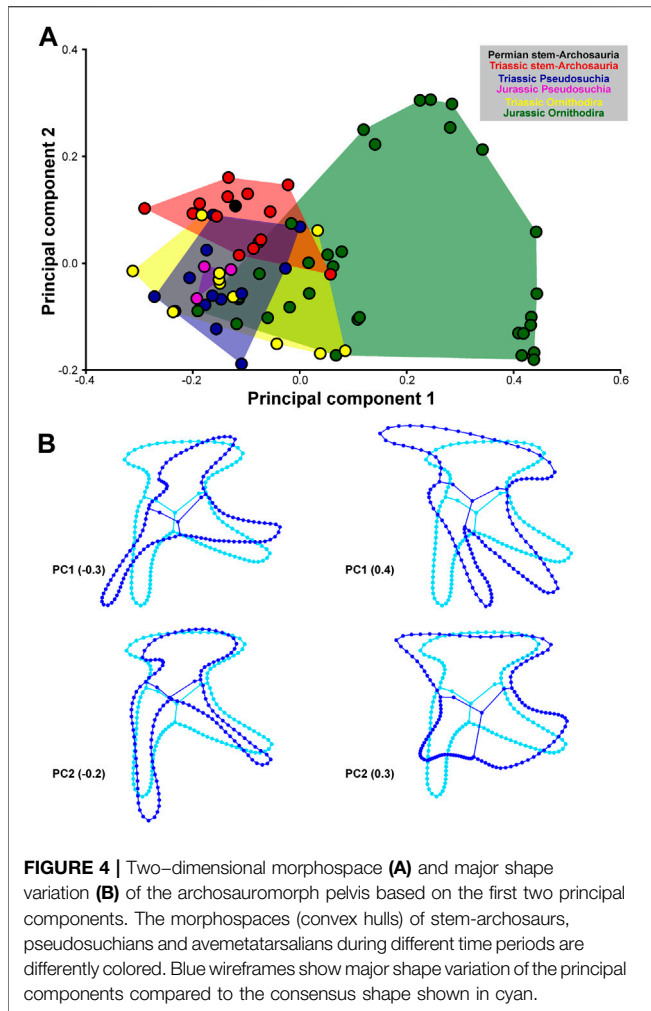


FIGURE 4 | Two-dimensional morphospace (A) and major shape variation (B) of the archosauromorph pelvis based on the first two principal components. The morphospaces (convex hulls) of stem-archosaurs, pseudosuchians and avemetatarsalians during different time periods are differently colored. Blue wireframes show major shape variation of the principal components compared to the consensus shape shown in cyan.

RESULTS

Cranial Morphospace

The first seven PCs contain significant shape variation based on the broken-stick method and account together for 80.1% of the total variation (PC1: 33.9%; PC2: 15.0%; PC3: 9.9%; PC4: 9.2%; PC5: 5.0%; PC6: 4.0%; PC7: 3.1%).

Negative values of PC1 describe dorsoventrally deep crania with a short rostrum, large subcircular orbit, deep suborbital jugal region, and anteroposteriorly long temporal region. Positive values of PC1 describe dorsoventrally flattened crania with a long rostrum due to an anteroposteriorly elongated premaxilla, relatively small subcircular orbit, low suborbital jugal region, and short temporal region. Negative values of PC2 describe dorsoventrally flattened crania with a long rostrum (including the antorbital fenestra) due to an anteroposteriorly elongated maxilla, a dorsally concave nasal region, large and subcircular orbit, a very low suborbital jugal region, and a ventrally located jaw joint. Positive values of PC2 describe dorsoventrally deep crania, with a short and dorsally convex rostrum (including a short and dorsoventrally deep antorbital fenestra), large and

suboval orbit, a deep suborbital jugal region, and a ventrally located jaw joint (Figure 2). Negative values of PC3 describe crania with an anteroposteriorly long premaxilla and short maxilla, which are angled to each other along the ventral margin, small antorbital fenestra, flattened postrostral skull roof, small and subcircular orbit, deep suborbital jugal region, large lateral temporal fenestra, and a ventrally located jaw joint. Positive values of PC3 describe crania with an anteroposteriorly short premaxilla and long maxilla, large antorbital fenestra, high postrostral skull roof, large and suboval orbit, low suborbital jugal region, short infratemporal fenestra, and ventrally located jaw joint. Negative values of PC4 describe crania with a tapering snout as a result of an anteroposteriorly long premaxilla and short maxilla, small antorbital fenestra, anterodorsally inclined

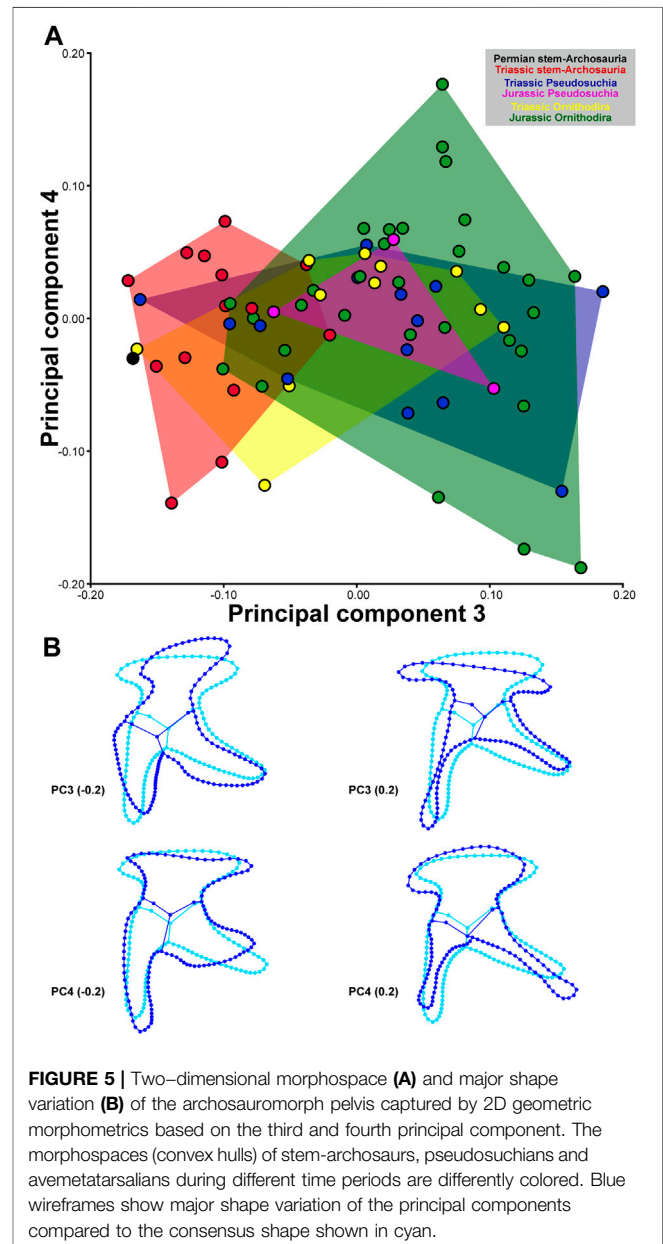


FIGURE 5 | Two-dimensional morphospace (A) and major shape variation (B) of the archosauromorph pelvis captured by 2D geometric morphometrics based on the third and fourth principal component. The morphospaces (convex hulls) of stem-archosaurs, pseudosuchians and avemetatarsalians during different time periods are differently colored. Blue wireframes show major shape variation of the principal components compared to the consensus shape shown in cyan.

suborbital jugal region, anteroposteriorly long temporal region, and ventrally located jaw joint. Positive values of PC4 describe crania with blunt snouts with an anteroposteriorly short premaxilla and long maxilla, large antorbital fenestra, suboval orbit, anteroventrally inclined suborbital region, and ventrally located jaw joint (**Figure 3**).

Stem-archosaurs, avemetatarsalians, and pseudosuchians strongly overlap with each other in the morphospace generated by the first four PCs, with the former showing a stronger overlap with avemetatarsalians on PC2 (**Figure 2**) and with pseudosuchians on PC3 (**Figure 3**).

Pelvic Morphospace

The first four PCs contain significant shape variation and account together for 83.5% of the total variation (PC1: 51.0%; PC2: 17.6%; PC3: 10.0%; PC4: 4.8%).

Negative values of PC1 describe pelves with an anteroventrally-to-posterodorsally inclined ilium that has a short preacetabular process and a long pubic peduncle; the pubis is elongated and anteroventrally directed (propubic) and the puboischiadic plate is dorsoventrally short; and the ischium is posteriorly directed. Positive values of PC1 describe pelves with an anteroventrally-to-posterodorsally inclined ilium that has a long preacetabular process, and a short pubic peduncle; the pubis is short and posteroventrally directed (opisthopubic) and has a prominent puboischiadic plate; and the ischium is posteroventrally directed. Negative values of PC2 describe pelves with an anteroposteriorly short ilium that has a short, blunt preacetabular process and anteroventrally directed pubic peduncle; the pubis is long, slender, and ventrally directed (isopubic), with a very short puboischiadic plate; and the ischium is long and slender. Positive values of PC2 describe pelves with an anteroposteriorly long ilium that has a long, tapering preacetabular process and ventrally directed pubic peduncle; the pubis is short and anteroventrally directed, with a long puboischiadic plate; and the ischium is short and broad, and posteriorly directed (**Figure 4**). Negative values of PC3 describe pelves with an anteroposteriorly short ilium that is anteroventrally-to-posterodorsally inclined, with a long, anteroventrally directed pubic peduncle, and where the acetabulum is relatively large; the pubis is short and posteroventrally directed (opisthopubic); and the ischium is short and broad. Positive values of PC3 describe pelves with an anteroposteriorly orientated ilium, with a dorsoventrally low blade, long preacetabular process, short pubic peduncle, and small acetabulum, a pubis with an anteroventrally directed (propubic), long and slender shaft and with expanded distal end, and a slender ischium. Negative values of PC4 describe pelves with an ilium with a short, tapering preacetabular process, long and slender postacetabular process, concave dorsal margin of the iliac blade, and short pubic peduncle; the pubis is long and ventrally directed (isopubic) and possesses a long puboischiadic plate; the ischium is short, broad, and posteriorly directed. Positive values of PC4 describe pelves with an ilium with a long, blunt preacetabular process, short, blunt postacetabular process, convex dorsal margin of iliac blade, and long pubic peduncle; the pubis is short and anteroventrally directed

(propubic), and possesses a very short puboischiadic plate; the ischium is long, slender, and posteroventrally directed (**Figure 5**).

As is the case for the cranium, stem-archosaurs, pseudosuchians, and avemetatarsalians overlap with each other in the pelvic morphospace generated by the four PCs, but the avemetatarsalian subclades Pterosauria and Ornithischia occupy more distant regions of the morphospace (**Figures 4,5**).

Major Patterns in Cranial Disparity

The general description of cranial disparity is based on sum of variances. The average nearest neighbor distance shows similar temporal trends and, as a result, we only report differences between these two metrics. The results for average displacements are described separately at the end of the section (**Figures 6–9; Supplementary File S1-Tables S4–S6**).

The cranial sum of variances of all archosauromorphs (including stem and crown archosaurs) increases from the late Permian to its maximum in the late Norian, only interrupted by a small reduction in the early Norian. After its peak, sum of variances decreases until the Hettangian and stays approximately constant until the Middle Jurassic. A minor increase occurs in the Late Jurassic, but without reaching the levels of the late Norian. Average nearest neighbor distance has a general increase from the late Permian to late Norian, but it is interrupted by a plateau during the late Middle Triassic to early Norian. Average nearest neighbor distance follows a similar pattern to sum of variances during the Jurassic (**Figure 6A**). For stem-archosaurs (i.e. non-archosaurian archosauromorphs), sum of variances increases from the late Permian to the early Norian, before it declines slightly in the late Norian (the last datapoint); this final decline is not present for the average nearest neighbor distance (**Figure 6B**).

In contrast, the sum of variances of crown archosaurs resembles major temporal trends found for all archosauromorphs, showing an initial increase from the late Permian to the late Norian (although with no decrease in the early Norian), followed by a decline in the Rhaetian. During the Early and Middle Jurassic, sum of variances shows a slight continuous increase, but it increases more conspicuously during the Late Jurassic and at that point it exceeds the late Norian local peak. The average nearest neighbor distance shows a minor interruption of this overall trend of increase during the early Norian, the increase peaks around the Triassic-Jurassic boundary, and declines in the Pliensbachian, subsequently increasing again during the Late Jurassic to similar values to those around the Triassic-Jurassic boundary (**Figure 6C**).

Within crown archosaurs, the sum of variances for pseudosuchian crania increases from the Early Triassic, reaching its peak in the late Norian, and stagnates until the end of the Triassic. After the Triassic-Jurassic mass extinction, the sum of variances decreases markedly, with minimum values from the Sinemurian to the Pliensbachian. Subsequently, disparity increases constantly until the Late Jurassic, but without reaching the late Norian values. The average nearest neighbor distance stagnates from the Carnian to the early Norian, and peaks in the Rhaetian. Across the Triassic-Jurassic boundary, this

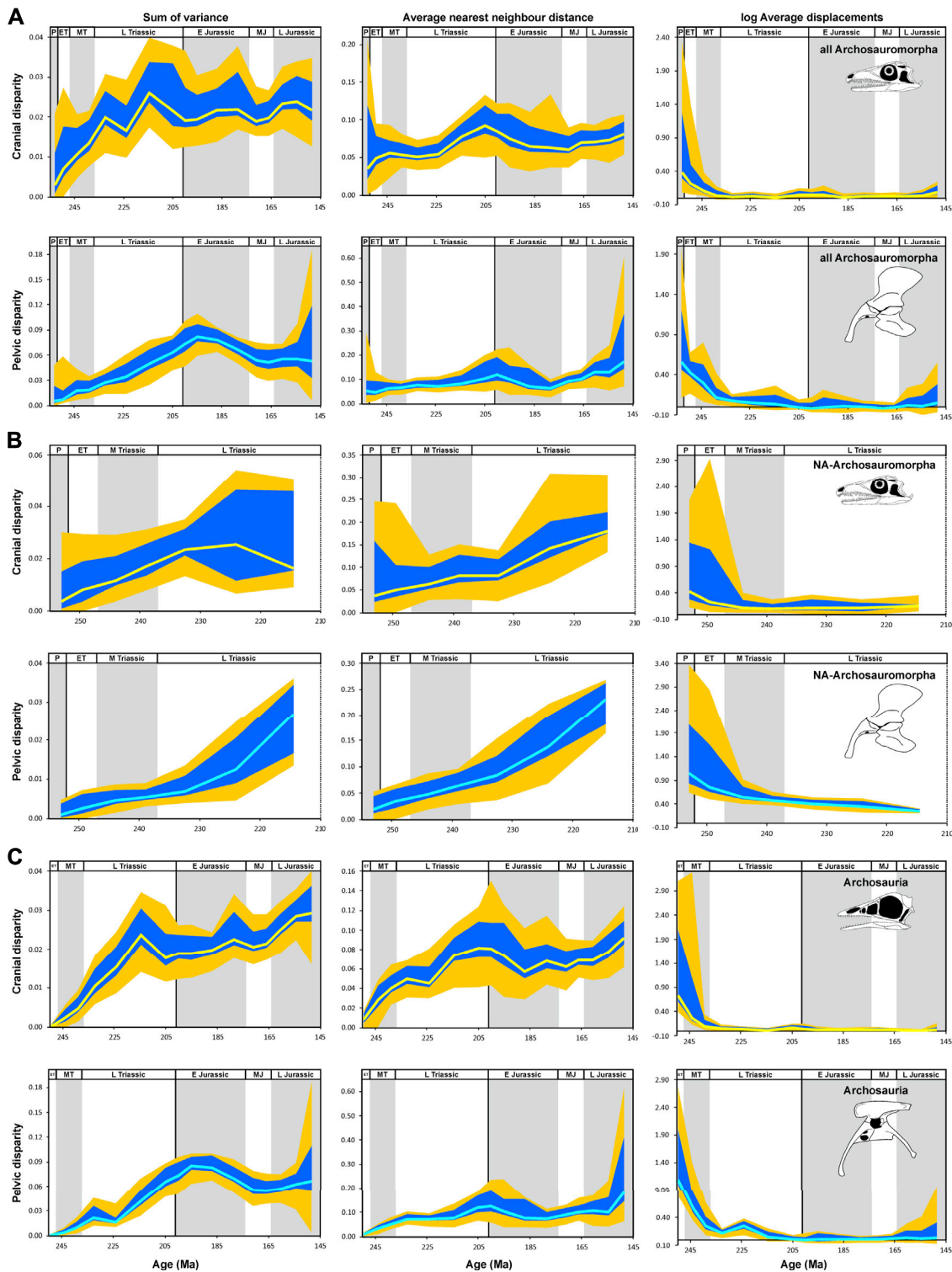


FIGURE 6 | Temporal disparity of archosauromorph cranium and pelvis captured by 2D geometric morphometrics from the late Permian to the Late Jurassic, as measured from phylogenetically interpolated values (“gradualistic” model), with disparity quantified as the sum of variances, average nearest neighbor distance and average displacements (log-transformed) based on shape variables of the principal component analysis. **(A)** Cranial and pelvic disparity of all archosauromorphs. **(B)** Cranial and pelvic disparity of non-archosaurian archosauromorphs (stem-archosaurs). **(C)** Cranial and pelvic disparity of crown-archosaurs. The yellow (cranium) and cyan (pelvis) solid lines show the median of estimated disparity for each bin, with the orange bands showing the total range of disparity estimated from 1,000 time-calibrated trees and the blue band showing the range delimited by the 2.5 and 97.5% quantiles of the same. *Prolacerta* skull **(A,B)** modified after Ezcurra (2016); *Archaeopteryx* skull **(C)** modified after Rauhut (2014); *Coelophysis* pelvis **(C)** modified after Tykoski (2005). Abbreviations: P, Permian; ET, Early Triassic; MT Middle Triassic L Triassic, Late Triassic; E Jurassic, Early Jurassic; MJ, Middle Jurassic; L Jurassic, Late Jurassic **(Supplementary Material S1-Tables S4–S6)**.

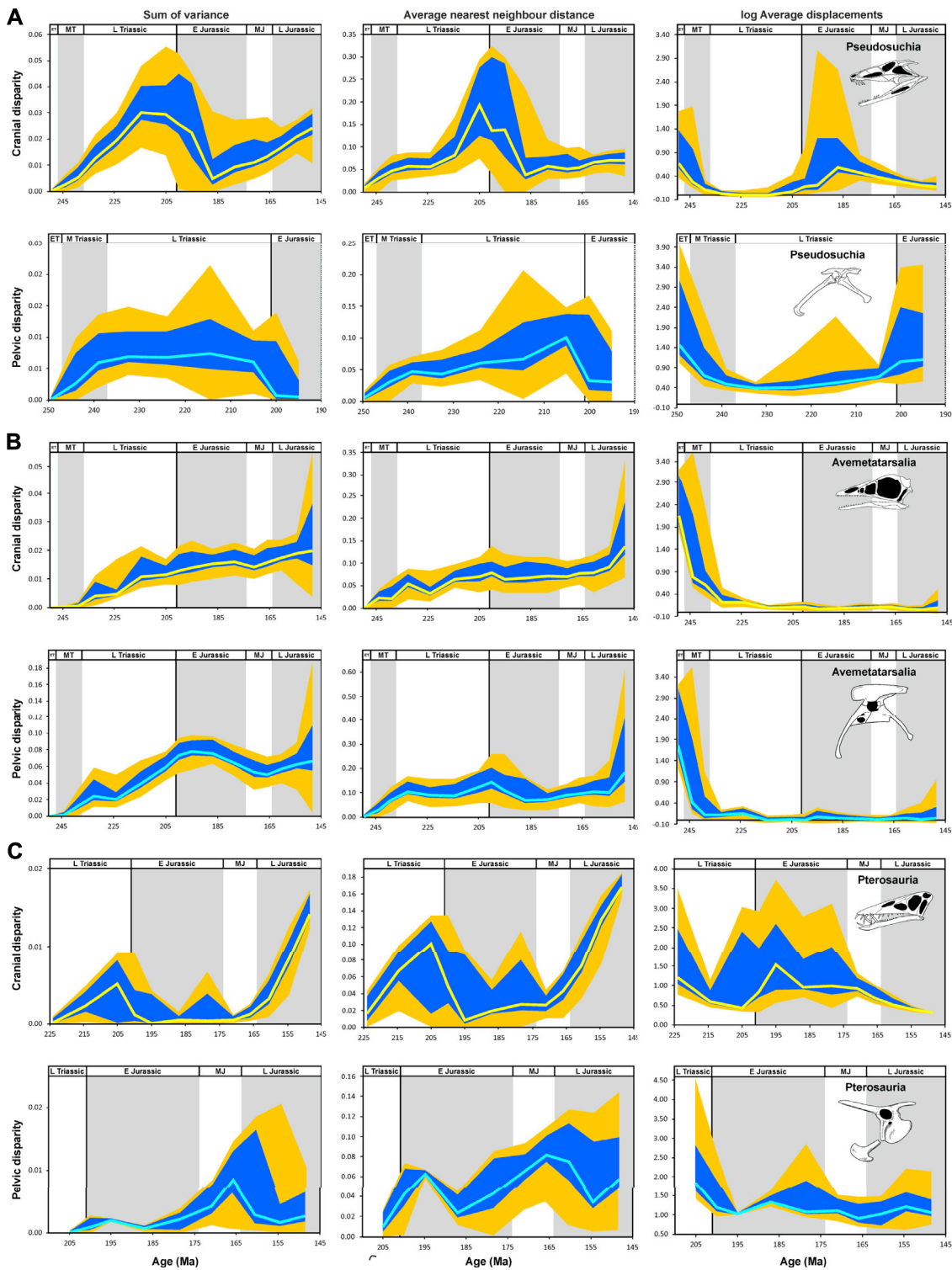


FIGURE 7 | Temporal disparity of archosauromorph cranium and pelvis captured by 2D geometric morphometrics from the late Permian to the Late Jurassic, as measured from phylogenetically interpolated values (“gradualistic” model), with disparity quantified as the sum of variances, average nearest neighbor distance and average displacements (log-transformed) based on shape variables of the principal component analysis. **(A)** Cranial and pelvic disparity of pseudosuchians. **(B)** Cranial and pelvic disparity of aemetatarsalians. **(C)** Cranial and pelvic disparity of pterosaurs. The yellow (cranium) and cyan (pelvis) solid lines show the median of estimated disparity for each bin, with the orange bands showing the total range of disparity estimated from 1,000 time-calibrated trees and the blue band showing the range delimited by the 2.5 and 97.5% quantiles of the same. *Erpetosuchus* skull **(A)** modified after Benton and Walker (2002); *Poposaurus* pelvis **(A)** modified after Schachner et al. (2011); *Archaeopteryx* skull **(B)** modified after Rauhut (2014); *Coelophysis* pelvis **(B)** modified after Tykoski (2005); *Dorygnathus* skull and pelvis **(C)** modified after Wellnhofer (1978). Abbreviations: P, Permian; ET, Early Triassic; MT Middle Triassic L Triassic, Late Triassic; E Jurassic, Early Jurassic; MJ, Middle Jurassic; L Jurassic, Late Jurassic **(Supplementary Material S1-Tables S4–S6)**.

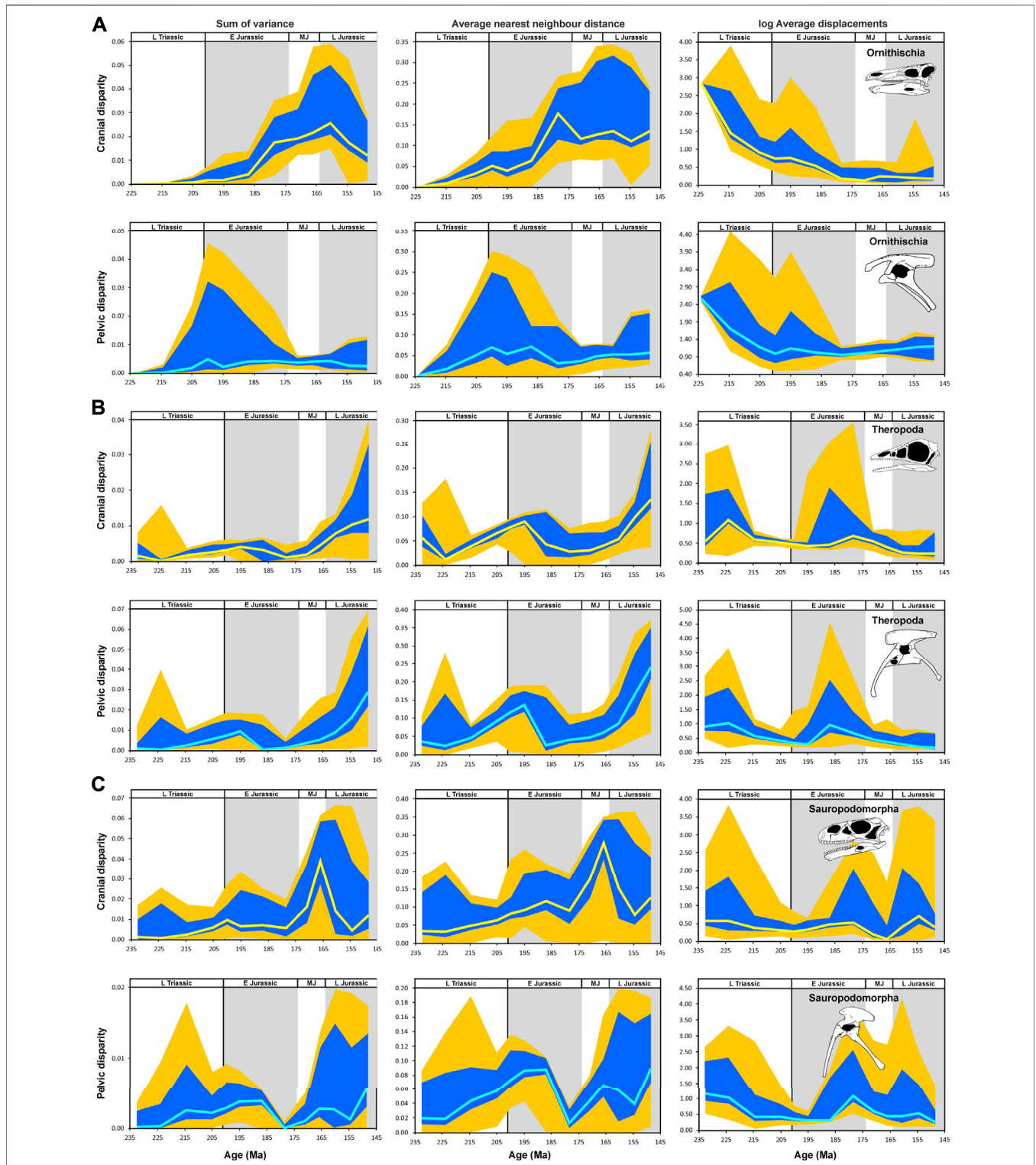


FIGURE 8 | Temporal disparity of archosauromorph cranium and pelvis captured by 2D geometric morphometrics from the late Permian to the Late Jurassic, as measured from phylogenetically interpolated values (“gradualistic” model), with disparity quantified as the sum of variances, average nearest neighbor distance and average displacements (log-transformed) based on shape variables of the principal component analysis. **(A)** Cranial and pelvic disparity of ornithischians. **(B)** Cranial and pelvic disparity of theropods. **(C)** Cranial and pelvic disparity of sauropodomorphs. The yellow (cranium) and cyan (pelvis) solid lines show the median of estimated disparity for each bin, with the orange bands showing the total range of disparity estimated from 1,000 time-calibrated trees and the blue band showing the range delimited by the 2.5 and 97.5% quantiles of the same. *Stegosaurus* skull **(A)** modified after Sereno and Dong (1992); *Scelidosaurus* pelvis **(A)** modified after Carpenter (2013); *Archaeopteryx* skull **(B)** modified after Rauhut (2014); *Coelophysis* pelvis **(B)** modified after Tykoski (2005); *Adeopapposaurus* **(C)** modified after Martínez (2009); *Eoraptor* pelvis **(C)** modified after Sereno et al. (2013). Abbreviations: P, Permian; ET, Early Triassic; MT Middle Triassic L Triassic, Late Triassic; E Jurassic, Early Jurassic; MJ, Middle Jurassic; L Jurassic, Late Jurassic **(Supplementary Material S1-Tables S4–S6)**.

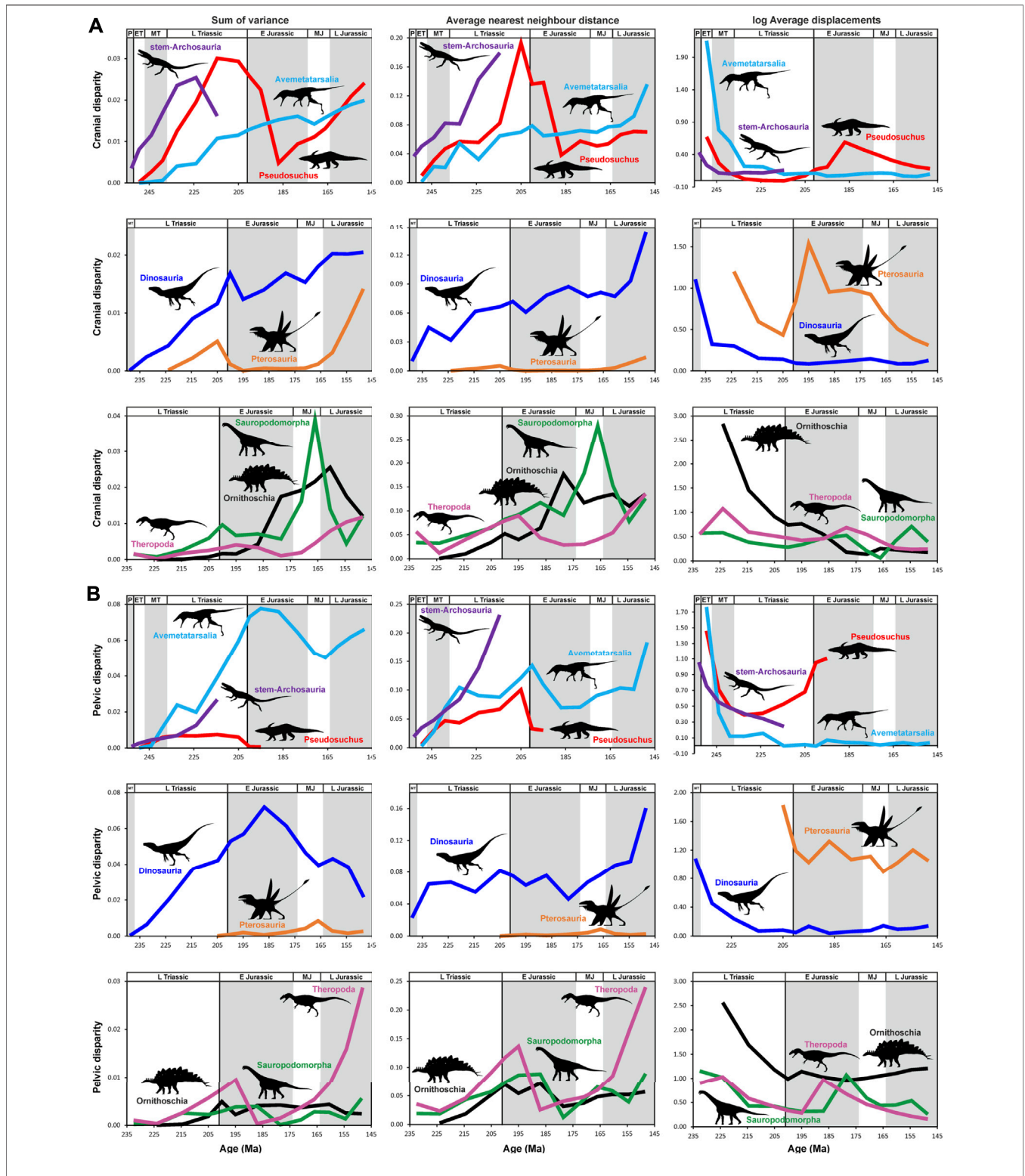


FIGURE 9 | Comparison of median cranium and pelvis disparity captured by 2D geometric morphometrics from the late Permian to Late Jurassic between different archosauromorph groups, as measured from phylogenetically interpolated values (“gradualistic” model), with disparity quantified as the sum of variances, average nearest neighbor distance and average displacements (log-transformed) based on shape variables of the principal component analysis. **(A)** Cranial disparity of stem-archosaurs (dark purple line), pseudosuchians (red line), avemetatarsalians (cyan line), dinosaurs (blue line), pterosaurs (orange line), ornithischians (black line), theropods (magenta line) and sauropodomorphs (green line). **(B)** Pelvic disparity of stem-archosaurs (dark purple line), pseudosuchians (red line), avemetatarsalians (cyan line), dinosaurs (blue line), pterosaurs (orange line), ornithischians (black line), theropods (magenta line) and sauropodomorphs (green line). All silhouettes taken from (www.phylopic.org). Abbreviations: P, Permian; ET, Early Triassic; MT Middle Triassic L Triassic, Late Triassic; E Jurassic, Early Jurassic; MJ, Middle Jurassic; L Jurassic, Late Jurassic (**Supplementary Material S1-Tables S4-S6**).

curve drops until the Pliensbachian, showing only a minor recovery afterwards (**Figure 7A**).

In contrast, *Avetatarsalia* shows an approximately constant increase of sum of variances from the late Permian to the Late Jurassic. The same trend is found for average nearest neighbor distance, but with a stronger increase during the Late Jurassic (**Figure 7B**).

Interpolating shape variation along the branches also allows assessment of patterns for subclades that otherwise could not be investigated due to their small sample sizes (although the smaller sample sizes and phylogenetic uncertainty likely increase error). In this regard, the sum of variances of pterosaur crania increases from the late Norian to the Rhaetian, followed by a strong drop at the Triassic-Jurassic boundary until the Sinemurian. The curve remains low until the end of the Middle Jurassic before it increases exceptionally fast during the Late Jurassic. This pattern is also found for average nearest neighbor distance, but with a gradual increase during the Early Jurassic (**Figure 7C**).

The cranial disparity of dinosaurs follows approximately the patterns described for *Avetatarsalia*. For ornithischian crania, sum of variances remains low during the whole Late Triassic and the first half of the Early Jurassic. From the Pliensbachian onwards, sum of variances increases until the Oxfordian, but drops towards the Tithonian. The average nearest neighbor distance shows a stronger increase during the Triassic. The curve peaks in the Toarcian and drops slightly in the Middle Jurassic, before entering a period of stagnation until the end of the Late Jurassic (**Figure 8A**).

From the Late Triassic to the Middle Jurassic, the sum of variances is low for theropod dinosaurs, after which it strongly increases until the end of the Late Jurassic. The average nearest neighbor distance increases from the early Norian to the Sinemurian. After a small decrease, the curve increases from the Middle Jurassic until the Late Jurassic (**Figure 8B**).

The sum of variances of sauropodomorphs shows a low, gradual increase from the Late Triassic to the end of the Late Jurassic, with a small peak during the Hettangian and a second much higher peak in the late Middle Jurassic. The average nearest neighbor distance increases constantly, and more abruptly than sum of variances, from the Late Triassic to the Pliensbachian, followed by an extreme late Middle Jurassic peak, as occurs with the sum of variances (**Figure 8C**). Dinosauria as a whole shows a steady increase in cranial disparity from the Late Triassic to the Late Jurassic (**Supplementary File S1-Tables S4–S6**).

The samples of all archosauromorph, stem-archosaur, crown-archosaur, *avetatarsalian*, and dinosaur crania show a similar trend for the average displacement, with approach to the centroid of the morphospace (denoted by a diminution of the metric) following their time of origin followed by a long period of stagnation close to the centroid. For pseudosuchians, this pattern is also seen during the Triassic, but some notable distancing from the centroid occurring from the Rhaetian to the Pliensbachian. Thereafter, pseudosuchians became progressively closer to the centroid of the morphospace until the end of the Late Jurassic, but occupying a more distant position to the centroid than in the Late Triassic. Pterosaurs also show a similar trend of approach to the centroid during the Triassic, but

occupy a more distant position from the centroid than all archosauromorphs together and all non-dinosaurian archosauromorph groups. Subsequently, pterosaurs pass through a period of distancing from the centroid from the Rhaetian to the Sinemurian, before approaching the centroid again to reach the lowest distance at the end of the Late Jurassic. For ornithischians, the period of approach to the centroid is prolonged, spanning from the early Norian to the Toarcian, before stagnation relatively close to the centroid until the youngest sampled time bin. Theropod dinosaurs show a minor distancing from the centroid from the Carnian to the early Norian, and thereafter there is a gradual convergence towards the centroid. A second distancing from the centroid occurs during the Toarcian, before the theropod morphospace becomes closer to the centroid once again. The average displacement curve of sauropodomorphs is approximately constant from the Carnian to the end of the Early Jurassic, with a position relatively distant from the centroid. During the Middle Jurassic, the morphospace of sauropodomorphs becomes closer to the centroid and then departs again in the Late Jurassic (**Figures 6–8; Supplementary File S1-Tables S4–S6**).

Major Patterns in Pelvic Disparity

The pelvic sum of variances of all Archosauromorpha increases constantly from the late Permian up to a maximum in the Sinemurian. Subsequently, the sum of variances approximately halves by the end of the Middle Jurassic and stagnates at this level until the end of the Late Jurassic. The average nearest neighbor distance is approximately constant until the end of the Early Jurassic, showing a minor peak in the Hettangian, and then increases from the Toarcian until the end of the Late Jurassic (**Figure 6A**).

For stem-archosaurs, sum of variances and average nearest neighbor distance continuously increase from the late Permian until the late Norian (the last data point), with an increase of rate of increase during the Late Triassic (**Figure 6B**).

The course of sum of variances through time in crown archosaurs resembles that for all archosauromorphs, differing only in that there is a minor decrease during the early Norian and a small increase during the Late Jurassic. The average nearest neighbor distance increases from the Early Triassic to Carnian and remains approximately constant until the Kimmeridgian, with a minor peak around the Triassic-Jurassic boundary. The curve ends with an increase during the Tithonian (**Figure 6C**).

The sum of variances of pseudosuchian pelvises increases from the Early Triassic until the Carnian, followed by a period of stagnation until the end of the Triassic. At the Triassic-Jurassic boundary, a marked drop is observed, but due to lack of data the course of disparity cannot be traced further than the Sinemurian. The average nearest neighbor distance shows a quite similar pattern with a peak during the Rhaetian (**Figure 7A**).

The temporal patterns of sum of variances and average nearest neighbor distance in *avetatarsalians* are almost identical to those of crown archosaurs as a whole (**Figure 7B**). The sum of variances of the pterosaur pelvises remains low from the Late Triassic to the end of the Late Jurassic, showing a high local peak in the late Middle Jurassic. The average nearest neighbor distance

increases from the Rhaetian to the Sinemurian and drops during the Pliensbachian. Thereafter, it increases until the end of the Middle Jurassic before dropping again in the middle Late Jurassic (**Figure 7C**).

The sum of variances of dinosaur pelvises increases constantly from the Late Triassic to the Pliensbachian, followed by a steady drop until the end of the Jurassic. The average nearest neighbor distance shows a small initial increase during the Carnian and remains constant until the Kimmeridgian, showing a final increase during the Tithonian. The sum of variances for ornithischian pelvis is low over the entire studied interval, with a minor peak around the Triassic-Jurassic boundary. The average nearest neighbor distance shows an increase from the early Norian to the Hettangian and stagnates until the Pliensbachian. Towards the end of the Early Jurassic, the average nearest neighbor distance decreases, but shows a slow and steady recovery until the end of the Late Jurassic (**Figure 8A**). The sum of variances and average nearest neighbor distance of the theropod pelvises increase steadily from the Late Triassic to the Sinemurian, followed by a marked drop in the Pliensbachian, and a pronounced rebound lasting until the end of the Late Jurassic (**Figure 8B**). The sum of variances of sauropodomorph pelvises increases slowly from the Late Triassic to the Pliensbachian, followed by a pronounced drop in the Toarcian and a subsequent increase until the end of the Late Jurassic. The average nearest neighbor distance shows the same major trends (**Figure 8C**).

The samples of all archosauromorph, stem-archosaur, crown-archosaur, avemetatarsalian, dinosaur, pterosaur, and ornithischian hips show a similar trend for the average displacement with an initial approach towards the centroid after their time of origin and a long period of stagnation close to the centroid of the morphospace. For pseudosuchians, the trend is similar for the Triassic, but it shows the exploration of new regions of the morphospace in the Early Jurassic. Theropod dinosaurs show displacements away from the centroid in the Carnian to the early Norian. Thereafter, the sample of theropod hips stagnates relatively far from the centroid and shows a second notable movement away from the centroid during the Toarcian. Sauropodomorphs approach the centroid from the Carnian to the late Norian and stagnate until the Pliensbachian, followed by a major movement away from the centroid in the Toarcian and thereafter another movement towards the centroid during the Middle and Late Jurassic (**Figures 6–8; Supplementary File S1-Tables S4–S6**).

Regression Analyses

In a few of the clades examined, disparity through time correlates significantly with sampled diversity (**Supplementary File S1-Table S7**). Cranial sum of variances correlates significantly with sampled diversity in Archosauromorpha and Archosauria as a whole, while pelvic sum of variances correlates with disparity in stem-archosaurs and ornithischians. No significant correlations were detected between average nearest neighbor distance and sampled diversity for the cranial dataset, and a significant correlation was only found for stem-archosaurs for the pelvic dataset. In the case of the average displacements,

correlations between this metric and sampled diversity are more frequent, occurring for all archosauromorphs, archosaurs, pseudosuchians, avemetatarsalians, dinosaurs, and pterosaurs for the cranial dataset, and archosaurs, pseudosuchians, avemetatarsalians, ornithischians, and pterosaurs for the pelvic dataset.

Tests for correlations between the disparity metrics of the cranial and pelvic datasets with each other through time were significant for several clades (**Supplementary File S1-Table S8**). Sum of variances for cranium and pelvis shows significant correlations for all Archosauromorpha, Avemetatarsalia, and Theropoda, whereas average nearest neighbor distances show significant correlations for all clades with the exception of Ornithischia, Sauropodomorpha and Pterosauria. The average displacement values of the cranial and pelvic datasets retrieved significant correlations for almost all clades, with the exception of Sauropodomorpha and Pterosauria.

Evolutionary Rates

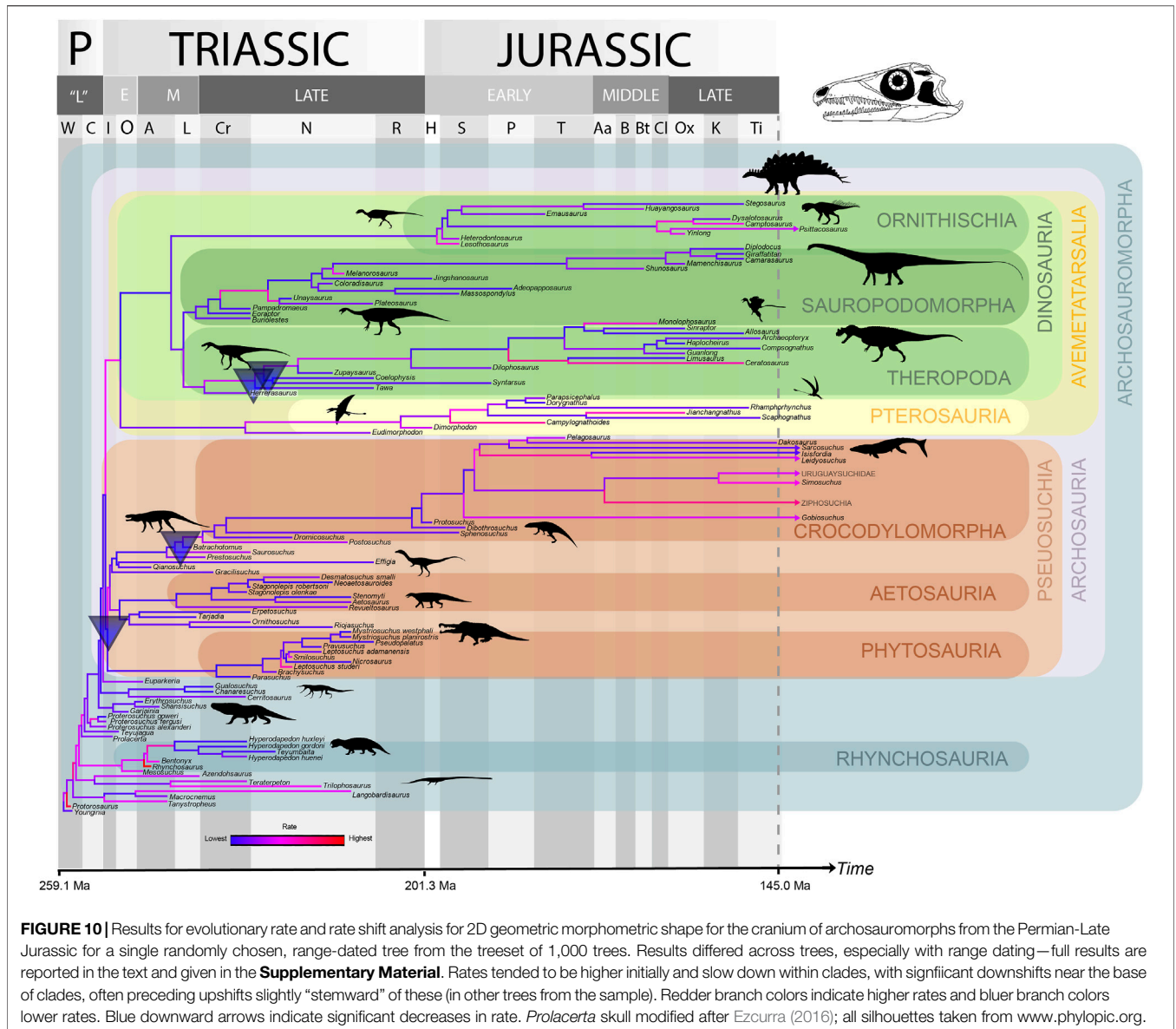
Evolutionary rates were faster at the beginning of the archosauromorph radiation than later in time (**Figures 10–12**), with a significant trend of decrease in rates through time for the pelvis using phylogenetic ridge regression across the whole tree (see **Supplementary File S1-Table S9**). There were no other significant trends in rate through time for any of the PC values (or for all taken together) for either the cranium or pelvis and the tree as a whole, but the slope was always negative except for PC3 in the pelvic data (see **Supplementary File S1-Table S9**). A number of significant shifts (i.e. significant changes of rate at particular nodes of the tree) in the rate of evolution of the cranium and pelvis were detected (see **Supplementary File S1-Table S10**), but these were strongly influenced by age uncertainties affecting the branch lengths, and also the tree topology. Shift locations also varied considerably among the range-dated trees.

Cranial Rate Shifts

Downshifts in cranial rates were detected in all trees somewhere within Pseudosuchia, usually near or at the base of the clade. A downshift was also detected in all trees usually at Avemetatarsalia (142 of the 1,000 analysed trees) or Dinosauria (29 trees) and at Theropoda (25 trees) or Neotheropoda (723 trees). A significant increase in rate was detected either at Saurischia (three trees) or near the base of Sauropodomorpha (129 trees) (**Figure 10**). Using non-allometric residuals, results were broadly similar, with an additional downshift detected at the *Prestosuchus* + Crocodylomorpha clade in two trees (see **Supplementary File S1-Table S10**).

Pelvis Rate Shifts

Shift detection results differed considerably from the cranial dataset. Overall, using range-dating, significant increases at the base of major clades were followed by significant decreases within clades, but there was some variation. A decrease at Dinosauromorpha was detected in 58 trees, followed by an increase around the base of Dinosauriformes (one tree) or Dinosauria (10 trees). A further increase was detected at



Ornithischia in 82 trees, and a decrease at the clade that includes *Heterodontosaurus* + other ornithischians was detected in 714 trees. Similarly, an increase at Sauropodomorpha was detected in 18 trees, and a decrease at the *Plateosaurus* + Sauropoda clade in 26 trees. In contrast, a decrease in rate was detected at Pseudosuchia (47 trees), and an increase in various early pseudosuchian clades (42 trees, differing exact clades) (**Figure 11**). Results were very similar using non-allometric residuals, with only the upshift at Dinosauriformes failing to be detected (see **Supplementary File S1-Table S10**).

Comparison of Rates and Change in Rates Between Groups and Rest of Tree

For the cranial dataset, Archosauria showed significantly lower rates (estimated marginal means—EMMs; $p < 0.05$) than the rest of the tree for PC3 (broadly speaking, a skull with smaller

and more dorsally-placed orbit and antorbital fenestra versus one with larger, more ventrally placed openings—see above). Significantly lower EMMs were also found for Dinosauria for PC3 and Pseudosuchia for PC2 (a long, low skull versus a high skull with tall rostrum—see above) compared to the rest of the tree, and the change in rate through time (slope) was significantly higher for Pseudosuchia for PC3. For the pelvic dataset, the rate for PC3 (a more robustly built “stem”-type pelvis versus a theropod-like gracile pelvis—see above) was significantly lower in Archosauria than in the rest of the tree using range dating. The change in rate through time for PC4 (a stockier, more robust pelvis as in some stem taxa and pseudosuchians versus a sauropod-type more gracile pelvis with curved iliac blade margin—see above) in Sauropodomorpha was also significantly higher than that for the rest of the tree using

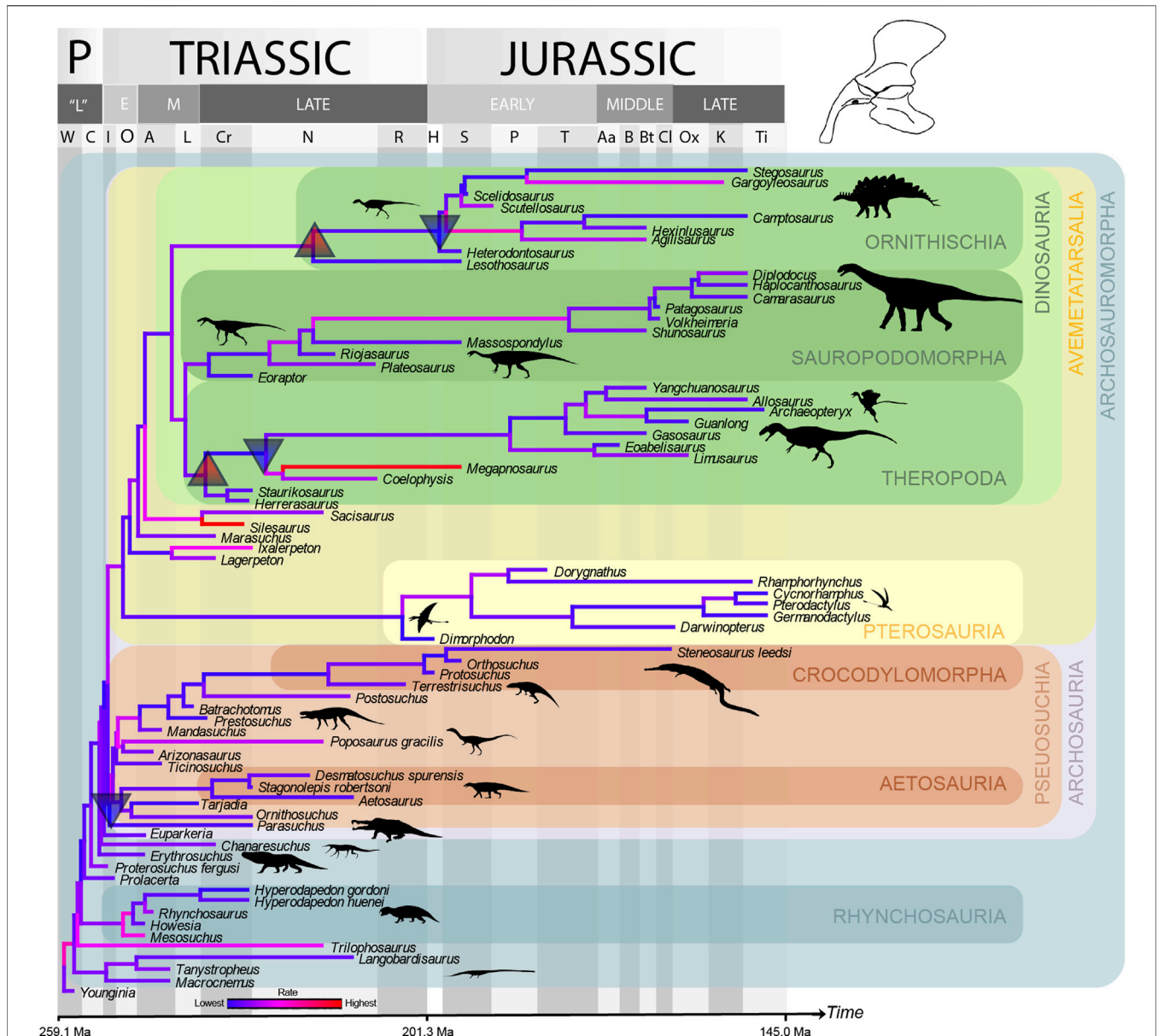


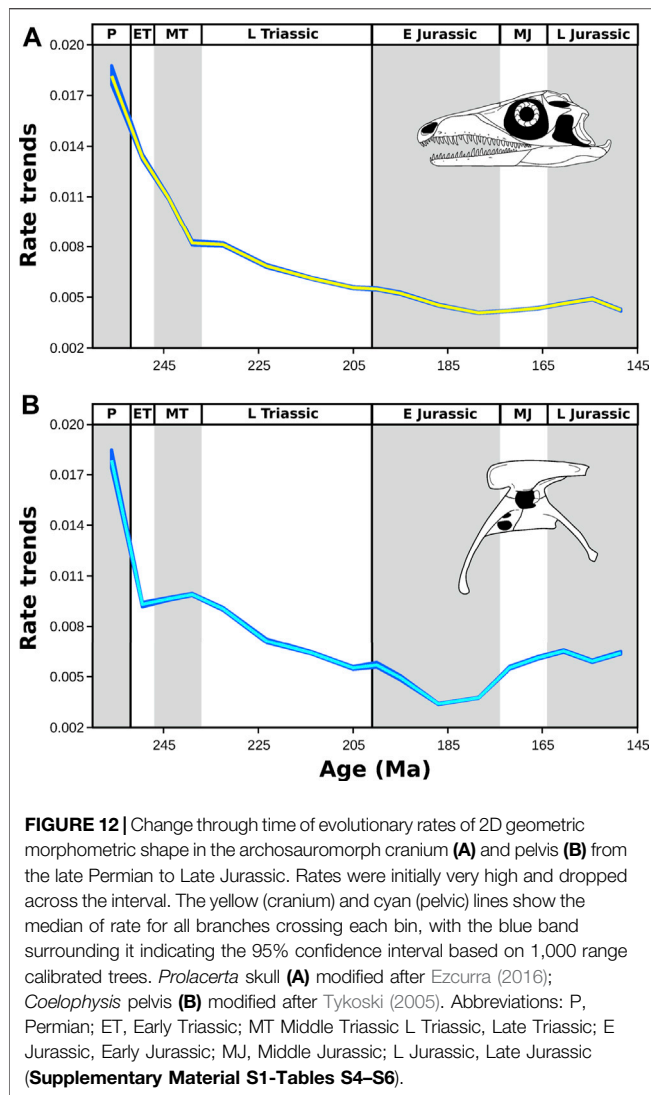
FIGURE 11 | Results for evolutionary rate and rate shift analysis for the pelvis for 2D geometric morphometric shape for archosauromorphs from the Permian-Late Jurassic for a single randomly chosen, range-dated tree from the treeset of 1,000 trees. Results differed across trees, especially with range dating—full results are reported in the text and given in the **Supplementary Material**. Rates tended to be higher initially and slow down within clades, with significant downshifts near the base of clades, often preceding upshifts slightly “stemward” of these. Redder branch colors indicate higher rates and bluer branch colors lower rates. Blue downward arrows indicate significant decreases in rate. All silhouettes taken from www.phylopic.org.

range dating. All other comparisons were non-significant (see **Supplementary File S1-Table S11**).

Rates Through Time

When the median cranial rate for all taxa is plotted through time there is a clear overall pattern of deceleration towards younger time bins. From the late Permian to the Ladinian, the rates decrease by more than half. After a short period of stagnation across the Middle-Late Triassic boundary, the median cranial rate decreases continuously, reaching

its minimum in the Toarcian, followed by a minor increase towards the end of the Late Jurassic (**Figure 12; Supplementary File S1-Table S12**). The median pelvic rate for all taxa shows a pattern broadly consistent with the cranium, including an initial global peak and a deceleration during the rest of the Triassic-Pliensbachian with an interruption around the Middle-Late Triassic boundary. Contrasting, however, with the cranial rate, pelvic rate accelerates in the late Early Jurassic and this pattern continues during the rest of the Jurassic (**Figure 12;**



Supplementary File S1-Table S12). There was a significant negative correlation between time and stage-binned median rate for the skull ($p < 0.01$) and the pelvis ($p < 0.001$) but this was reduced (skull; $p < 0.05$) or disappeared (pelvis; $p > 0.05$) using an autoregressive model (**Supplementary File S1-Table S12**). For the skull, a generalized random walk (GRW) model with a negative step mean ($-9.99e^{-5}$) fitted the mean stage-binned rate better than an unbiased random walk (URW; $\Delta AICc = 0.887$), whereas for the pelvis the URW was the better fit ($\Delta AICc = 1.251$), although the GRW step mean was also negative ($-1.12e^{-5}$). A correlation between the skull and pelvis median rates was significant ($p < 0.001$) and remained significant ($p < 0.01$) using an autoregressive model (**Supplementary File S1-Table S12**), supporting statistically the similar pattern shown by both skeletal partitions. The minor decoupling between the regions as a result of an acceleration in pelvic rates is reflected in the higher residual values of this regression in the last three time bins.

DISCUSSION

The results reported above provide a much more detailed and comprehensive picture of the early archosauromorph radiation than those of similar previous studies (e.g. Foth et al., 2016a) and have far-reaching implications both for this specific radiation and for the study of macroevolutionary radiations more broadly. They provide evidence of a delayed disparity peak in the archosauromorph radiation, similar to other larger radiations but contrasting with many taxonomically shallower or smaller ones, and of reducing rates of evolution through time concordant with an “early burst” pattern of evolution *sensu lato*. More specifically, this work also confirms previous elucidation of an underappreciated ecomorphological diversity in stem archosaur taxa, confirming the ecological importance of these species in Triassic terrestrial ecosystems, and demonstrates the benefits of including ghost/Lazarus lineages in studies of relatively poorly sampled clades.

Disparity Patterns in the Context of the Archosauromorph Radiation and Macroevolution

Evidence of a Delayed Peak in Disparity but “Early Burst” of Evolution

The sum of variances (volume) and average nearest neighbor distance (density) through time describe a broadly similar pattern in each of our datasets, which is congruent with the simulations of Guillaume et al. (2020). Using these two metrics, all sampled clades showed a delayed density-volume disparity peak in both the cranium and pelvis. Archosaurs (cranium), avemetatarsalians (cranium), dinosaurs (cranium), theropods (cranium and pelvis), sauropodomorphs (pelvis), and pterosaurs (cranium) all reach their maximum disparity at the end of the Jurassic, which is the last bin sampled. This indicates that disparity was not likely saturated by the end of the time span sampled here, and these trends of increase may continue in the Cretaceous. Similar delayed disparity peaks have been previously found for pterosaurs (Prentice et al., 2011; Butler et al., 2012; Foth et al., 2012), crocodylomorphs (Stubbs et al., 2021), and turtles (Foth and Joyce, 2016; Foth et al., 2017), but contrast with many smaller clades (see below). In contrast, concordant with our results for rates of change through time (see *Discussion* below), Archosauromorpha as a whole and all of the subclades examined (see specific points for Dinosauria, below) show broadly decreasing average displacement through time, indicating that evolutionary change tended to tail off after the initial radiation of novel ecomorphologies, concordant with an “early burst” pattern of evolution *sensu lato* (Puttick, 2018).

Pelvic Data Further Supports Underappreciated Stem Archosaur Disparity

At its highest peak, the cranial disparity of stem-archosaurs almost reaches the maximum values of Triassic pseudosuchians (**Figure 9**), as was previously reported by Foth et al. (2016a). While the sum of variances of the stem-archosaur cranial dataset already declines slightly towards the end of the

Norian, their pelvic disparity continued to rise until the end of the Triassic. Indeed, the pelvic disparity peak of stem-archosaurs is almost three times higher than that of pseudosuchians, pterosaurs, sauropodomorphs, and ornithischians when all these groups are considered separately (**Supplementary File S1-Tables S4–S6**). Thus, stem-archosaurs possessed an unappreciated disparity of hip morphologies, indicating a high diversity in terms of habitat preferences and locomotion styles (e.g. Renesto et al., 2002; Renesto and Saller, 2018; Ezcurra et al., 2021a). This supports previous work that demonstrated that stem taxa were diverse and successful (Foth et al., 2016a; see below). However, when compared with Avemetatarsalia and Dinosauria, stem-archosaurs have a lower sum of variances, but surpass the latter clades in their average nearest neighbor distance values (**Supplementary File S1-Tables S4–S6**).

The Triassic-Jurassic Mass Extinction and Major Reduction in Pseudosuchian Disparity

As described for the cranium, the pelvic volume-density disparity of pseudosuchians shows a strong decline across the Triassic-Jurassic boundary (see above), which may be related to the mass extinction event. However, due to the poor sampling of pseudosuchian pelvises in the Jurassic, this result should be treated with caution. However, this result agrees with conclusions of Toljagić and Butler (2013)—who investigated pseudosuchian disparity across the Triassic-Jurassic boundary based on discrete characters of the entire skeleton – that this extinction event affected primarily non-crocodylomorph pseudosuchians, while crocodylomorphs themselves radiated adaptively in the Early Jurassic, precipitating an increase in disparity and a shift in their morphospace occupation (see also Stubbs et al., 2021).

More surprisingly, the extension of the disparity analyses towards the end of the Jurassic reveals that after the decline in the Early Jurassic, the cranial disparity of pseudosuchians (represented by sum of variances) recovered in the Late Jurassic and surpassed that of avemetatarsalians. This increase in disparity is accompanied by a shift in morphospace and probably correlates with the adaptive radiation of crocodylomorphs in the Jurassic (Toljagić and Butler, 2013), when the clade radiated into a wide range of morphotypes with correspondingly varied cranial size and morphologies, including, for example, marine thalattosuchians, semi-aquatic goniopholidids, and terrestrial protosuchids (Bronzati et al., 2015; Mannion et al., 2015; Godoy et al., 2019; Stubbs et al., 2021). Only the terrestrial protosuchians were probably in direct competition with carnivorous avemetatarsalians, primarily small theropods.

Pterosaur Disparity and the Radiation of Monofenestrata/Pterodactyloidea

Within Avemetatarsalia, the cranial disparity of dinosaurs is clearly higher than that of pterosaurs during the entire study interval. Only in the Tithonian both groups approach one another as a consequence of the notable increase of cranial disparity in pterosaurs during the Late Jurassic. This increase in pterosaur disparity corresponds to major modifications in their

cranial anatomy, especially rostral adaptations for piscivory (Ösi, 2015). As we only sampled non-monofenestratan pterosaurs (for the cranial dataset; see *Materials and Methods*), which possess an external naris and antorbital fenestra as independent openings, we expect that the actual cranial disparity of pterosaurs was even higher than estimated here due to the radiation of Monofenestrata/Pterodactyloidea during the Middle and Late Jurassic (Lü et al., 2009; Andres et al., 2014). In contrast, pterosaurs possess an aberrant pelvic morphology compared to that of other archosauromorphs, possessing an ilium with an extremely elongated preacetabular process, a short, ventrally directed pubis, and a plate-like ischium (Wellnhofer, 1978), and their pelvic disparity is notably low when compared with dinosaurs. This reflects the greater variety of cursorial locomotor modes in dinosaurs (Carrano, 1999) and probable morphofunctional constraints imposed by flight in pterosaurs.

The Radiation of the Dinosauria and Disparity Patterns

Within Dinosauria, the increase of cranial and pelvic disparity is as a result of the early diversification of ornithischians, sauropodomorphs and theropods, probably concomitant with niche partitioning into herbivores (ornithischians, early sauropodomorphs, some theropods), megaherbivores (sauropods, some large bodied ornithischians), omnivores (some theropods, early sauropodomorphs and ornithischians), insectivores, carnivores, piscivores, and hypercarnivores (most theropods) (see Barrett and Rayfield, 2006; Barrett et al., 2011). Specialization for different food resources precipitated morphological diversification affecting the entire body plan, including the morphology of the skull and teeth, neck length, girdle and limb morphology, locomotion style, digestive system, and body size (e.g. Henderson, 2002; Sander et al., 2011; Barrett, 2014). Interestingly, however, the cranial and pelvic disparity of each main dinosaur group remains relatively low during the Late Triassic, while disparity curves for dinosaurs as a whole show a trend of increase. This indicates continued morphospace exploration by the clade as a whole, but relative stasis within morphotypes, which is in agreement with the results of the evolutionary rates analyses (see below). For the cranium, increase continues during the Jurassic for each main dinosaur clade. This may reflect a greater plasticity of the cranium and its adaptation to sub-niches within the broader morphospace of pelvic adaptation (see below).

Sauropodomorphs show the highest peak of cranial density-volume disparity among dinosaurs during the late Middle Jurassic. This peak could have been a result of the diversification of sauropods into two major clades during the Middle Jurassic, the Diplodocoidea, with relatively long rostra, and the Macronaria, with box-shaped crania. The peak is followed by a severe decline in sauropodomorph cranial disparity during the early Late Jurassic. However, the large confidence intervals for sauropodomorph disparity during the Middle Jurassic, which are caused by poor sampling, cast doubt on whether this decline was in fact as severe as it appears. In contrast, the cranial disparity of theropods displays a major increase later, during the Late Jurassic, probably reflecting the

diversification of the major lineages of the clade (Rauhut and Foth, 2020). Ornithischians show their strongest increase in cranial disparity during the late Early Jurassic, which is probably linked to the radiation of the three major ornithischian clades, Thyreophora, Ornithopoda and Marginocephalia, which all possess very distinct cranial morphologies (Weishampel et al., 2004). Thus, all dinosaur clades demonstrate a notable increase in cranial disparity during the Jurassic, which is consistent with the idea that the major ecomorphological radiation of dinosaurs occurred after the Triassic-Jurassic extinction event, when they filled many of the ecological niches left vacant by the extinction of other terrestrial amniotes (Benton, 1983; Brusatte et al., 2008a, 2010). Nevertheless, this ecomorphological diversification of dinosaurs seems to have occurred from the late Early Jurassic onwards, thus a many millions of years after the mass extinction event; thus, evidence of a direct replacement pattern as a consequence of empty niches left vacant by the extinction remains ambiguous.

The early increase of pelvic disparity seen in dinosaurs is probably linked to the appearance of the opisthopubic hip of ornithischians, which is one of the most aberrant forms within the pelvic morphospace. This pelvic morphology is probably related to a shift to an herbivorous diet (Weishampel and Norman, 1989; Barrett, 2014) that requires a longer intestinal tract for digestion (Chivers and Hladik, 1980). However, the pelvic disparity within ornithischians themselves is relatively low, and shows relatively little variation, which resembles the disparity pattern of the also highly aberrant pterosaur pelvis. Ornithischians have a complex evolutionary history in terms of locomotion, in which quadrupedality evolved at least three times independently from bipedal ancestors (Maidment and Barrett, 2012). While the shifts towards quadrupedality in ornithopods and marginocephalians occurred in the Cretaceous, the locomotory shift within thyreophorans falls within our study interval. However, in Thyreophora at least, this locomotor shift does not appear to be reflected in changes of pelvic disparity. Sauropodomorphs, which showed a similar dietary shift to that of ornithischians, did not evolve an opisthopubic pelvis, although later members show a mesopubic condition and probably solved the problem of digestion by increasing their body size (Sander et al., 2011). Like most ornithischians, sauropodomorphs also show a shift towards quadrupedality around the end of the Triassic (McPhee et al., 2018). Both ecological shifts fall into a period of disparity increase during the Norian and Early Jurassic. Thereafter, the pelvic disparity of sauropodomorphs fluctuates, with no clear pattern, with exception of a minor increase during the Late Jurassic. Theropods show an initial low peak in the Early Jurassic and a second major increase in pelvic disparity during the Late Jurassic. This latter peak is as a result of major differentiation between taxa affecting the shape of the preacetabular process, the orientation and curvature of the pubis, the shape and size of the pubic boot, the relative length and curvature of the ischium, and the shape and size of the ischial obturator process (Hutchinson, 2001).

Interestingly, the pelvic morphospace of Dinosauria as a whole declines steadily from the Pliensbachian to the end of the Late Jurassic based on density-volume disparity metrics, while each major dinosaur clade either stagnates (ornithischians), fluctuates (sauropodomorphs) or even increases (theropods) during this period. This discrepancy is explained by a shift in sauropodomorphs and theropods from propubic to mesopubic pelves, which resulted in a change of their morphospaces, moving closer to the opisthopubic ornithischian morphospace and decreasing the dinosaur morphospace occupation as a whole. These morphospace shifts for sauropodomorphs and theropods are indicated by peaks in the average displacement during the Jurassic and by high evolutionary rates (see below).

Disparity Patterns and Taxonomic Diversity

There is some evidence for a correlation between sampled diversity (i.e. number of observations per bin) and disparity, especially using the position metric (average displacement), which measures the average distance from the centroid. However, the density metric (average nearest neighbor distance) showed no significant correlation and the volume metric (sum of variances) showed very few, demonstrating the major impact that the chosen metric can have on the conclusions drawn. Average displacement is probably less likely to be influenced by outliers than sum of variances, with volume metrics often insensitive to unoccupied sections of trait space (Guillerme et al., 2020). On the other hand, average nearest neighbor distance is likely to underestimate disparity in the sample if it is composed of groups of closely-placed taxa, because the nearest neighbors will always be within these groups. It is in fact best considered as a measure of the quantity of measurements in trait space, and is therefore especially sensitive to sampling (Guillerme et al., 2020). Thus, in the context of comparison to sample size, average displacement may actually provide the most reliable metric when calculated for each group separately (as was the case here).

There does, thus, appear to be a quite common positive relationship between sampled diversity and disparity, as would be expected if taxa were effectively allotted randomly in trait space through unconstrained morphological evolution without a directional trend (Wesley-Hunt, 2005; Erwin, 2007). However, it is perhaps most revealing for which groups no correlation with average displacement is found, namely stem-archosaurs, Ornithischia, Theropoda and Sauropodomorpha for the cranial dataset, and all Archosauromorpha, stem-archosaurs, Dinosauria, Theropoda and Sauropodomorpha for the pelvic dataset. This perhaps reflects relatively conserved cranial morphologies in comparison to the mean within each dinosaur group during the sampled time interval, and a relatively conserved pelvic morphology in stem taxa and in dinosaurs except ornithischians.

The much more widespread lack of correlation of sampled diversity with the volume metric (sum of variances) is, as mentioned, probably at least partly due to development of very disparate morphologies failing to be matched by

sampling, i.e., due to unequal diversification of clades with different body plans (at least in the sample at hand—for example pterosaurs and ornithischians show relatively limited sampling but very disparate morphology—). The positive correlation found for Ornithischia when taken alone probably reflects the low diversity and low sampling (possibly null in the Triassic—Baron, 2019, but see Desojo et al., 2020) within the clade. The positive correlations for Archosauria and Archosauromorpha on the other hand probably reflect the large size of these clades both in disparity and diversity sampled, with the effects of outliers tending to be cancelled out. The lack of correlations with the density metric, average nearest neighbor distance, are far from surprising, because this will be strongly affected by unequal distribution of taxa in trait space and does not actually measure overall disparity, but rather the level of grouping in trait space.

Thus, especially at broad phylogenetic scale, our study does provide some evidence for a positive association between diversity and disparity, assuming that sampled diversity reflects taxonomic diversity. At first glance, this contrasts strongly with many previous studies for varied groups that have indicated that taxonomic and morphological diversity were decoupled (e.g. Wills et al., 1994; Fortey et al., 1996; Bapst et al., 2012; Marx and Fordyce, 2015; Puttick et al., 2020), with diversity often expanding or remaining high despite relatively low disparity (Benson et al., 2012; Ruta et al., 2013). However, these studies largely examined variance or range metrics, which—as discussed—are more likely to be affected by outliers. Our study thus demonstrates the utility and importance of comparing different potential measures of disparity. Evidence of a correlation even using the volume metric (sum of variances) at large phylogenetic scales also indicates that diversity and disparity may tend to be decoupled within radiations of ecomorphologically similar taxa (as in, for example, previous studies of plesiosaurs—Benson et al., 2012—or anomodont therapsids—Ruta et al., 2013), but correlate in clades showing broad ecomorphological diversity. Furthermore, there is some evidence that decoupling may become stronger later in time after an initial radiation, as rates decline (Brusatte et al., 2008b), some ecomorphologies are eliminated, but speciation continues (Schweizer et al., 2014), also perhaps explaining the correlations seen here.

The Effect of Including Ghost Lineages and Lazarus Taxa on Inference of Disparity Patterns

Measuring density-volume disparity exclusively from phylogenetically-interpolated shape variables results in curves that are much smoother than curves based on terminal taxa and hypothetical ancestors alone (Foth et al., 2017). However, when archosauromorph cranial disparity with interpolated phylogenetic relationships is compared with the results of Foth et al. (2016a), similar major patterns are recovered for all archosauromorphs, archosaurs, and avemetatarsalians. The course of the disparity curve for pseudosuchians during the Jurassic on the other hand differs considerably from that recovered by Foth et al. (2016a), but the same general pattern

of increase, decrease, and re-increase through time is still detected. A further difference when compared with Foth et al. (2016a) is the trajectory found for stem-archosaurs, probably due to the presence of several inferred ghost lineages (indicating the presence of Lazarus taxa) in the early Norian that were not taken into account in the previous study.

Nevertheless, major patterns are broadly similar to those found by Foth et al. (2016a), who did not include ghost lineages/Lazarus taxa: the Early and Middle Triassic is marked by a high cranial disparity of stem-archosaurs, pseudosuchians are the most disparate clade in the Late Triassic, and avemetatarsalians surpass pseudosuchians only in the Early Jurassic after the latter clade suffers a severe loss of disparity around the Triassic-Jurassic boundary (Figure 9; see also Brusatte et al., 2008a; Stubbs et al., 2013). The recovery of these broadly similar general disparity trends using interpolation of traits along branches indicates that the impact of Lazarus taxa in the late Permian and Early Triassic (i.e. Tanystropheidae, Allokotosauria, Erythrosuchidae) seems to be negligible. However, it should be noted that this concordance in disparity estimates may well relate to the already comprehensive sampling of stem-archosaurs in Foth et al. (2016a); and in the current study, and should only be generalized to similarly sampled groups.

In contrast, the cranial disparity of pterosaurs through time differs considerably from the results of Foth et al. (2012). This is not unexpected, however, because the latter study used only terminal taxa and an epoch-level coarse temporal binning instead of the stages used here. Nevertheless, the current study does reveal a small disparity peak at the end of the Late Triassic and a higher one at the end of the Late Jurassic, which broadly reflect the signal obtained by Foth et al. (2012). However, the latter study, due to its coarseness, misses an intermediate period of disparity depression between these peaks during the Early and Middle Jurassic. Thus, for groups with poorer sampling, the impact of including ghost lineages appears to be notably greater, and may allow further details of macroevolutionary patterns than otherwise detectable to be elucidated (see also Wilberg, 2017; Guillerme and Cooper, 2018).

Rates of Morphological Change Further Evidence for an “Early Burst” of Evolution in the Archosauromorph Adaptive Radiation

The results of our analyses of rates of morphological change for the tree as a whole are congruent with the disparity patterns of the average displacement (see above) and indicate a general pattern of morphological diversification with higher initial rates followed by lower rates once diversification into niches has occurred—an “early burst” pattern *sensu lato* (see below; Puttick, 2018). Major ecomorphological shifts, such as the development of herbivory, probably linked to the opisthopubic morphology in Ornithischia (see above; Weishampel and Norman, 1989; Barrett, 2014), appear to have been accompanied by high rates of morphological change. Reducing rates through time are seen in both the cranium and pelvis when fully incorporating phylogeny, but it is only for the pelvis that this trend is significant. This corresponds to a higher cranial than pelvic disparity in many archosauromorph groups (see above), and

may reflect lower lability of pelvic change than in cranial morphology, with fundamental pelvic changes occurring at the origin of clades (e.g. Ornithischia, Pterosauria) but followed by lower rates. This may indicate greater functional constraints on the pelvis because of its central role in locomotion, and lower necessity for change within particular dietary groups (e.g. larger and smaller carnivores). Cranial morphology on the other hand appears to remain more labile, with fluctuating changes in morphology probably related to specificity of diet. Furthermore, the origin of major ornithischian (ceratopsian, thyreophoran, ornithomorph) and pseudosuchian (thalattosuchian) morphotypes relatively late in the interval examined, in turn accompanied by major changes in cranial morphology, probably serves to reduce the temporal signal of decreasing rates; if the studied interval is extended forward in time, a statistically significant trend of decrease might be detectable. However, this pattern is no longer significant using non-allometric residuals, although the rate of pelvic evolution does still decline through time. Nevertheless, this does not in itself invalidate the conclusions drawn because body size is intimately connected to ecological niche and thus overall morphology; in this case, removal of allometric information may well in fact exclude important aspects of shape. Model fitting analysis using the mean stage-binned data, and regression of time against median stage-binned rate, both found evidence for a trend of decreasing rate through time for the skull. At first glance this contrasts with the results directly using phylogenetic ridge regression, but this can be considered to also support an early burst *sensu lato* pattern. This is because rates as a whole decrease over the interval, but this pattern is not consistent across the phylogeny because rates increase again at the base of some radiations and on particular lineages. Furthermore, stability in lineages following an initial early burst contributes to a pattern of overall decreasing rates when time-binned, but means that no significant trend of decrease is found for such lineages themselves when phylogeny is properly included because there is relative stability or even instances of increase later in the evolution of the lineages.

Location of Rate “Shifts”

The particular clades pinpointed as showing decreases and increases in rates were strongly affected by differences in tree dating and also (but to a lesser extent) by phylogenetic topology. However, these results also broadly support the idea of major morphological changes localized around the origins and radiations of major clades. Downshifts near the base of major clades indicate stabilising morphology within a radiating clade. Upshifts, though less consistently identified, tend—when they occur—to be located slightly “stemward” to downshifts in each clade, indicating high initial rates when major morphological innovation occurs and then a slowdown of rates as phylogenetic diversification of the clade takes place. For example, in the cranium, upshifts are detected around the base of Saurischia, but with subsequent slowdowns within Theropoda/Neotheropoda. An upshift around the base of Sauropodomorpha in some range-dated trees is not recovered when size-correlated aspects of shape are removed, and appears to be driven by the major increases in size in this lineage.

In the pelvis, this pattern was even more consistent, with increases at Dinosauromorpha (the clade that includes all taxa closer to the theropod dinosaur *Compsognathus*, than to the pterosaur *Pterodactylus* or the crocodile *Alligator*; see Ezcurra et al., 2020), Ornithischia, and Sauropodomorpha followed by subsequent decreases within each clade, respectively (**Supplementary File S1-Table S10**). This may reflect that pelvic changes are more extreme/fundamental than those in the cranium as new ecomorphologies are developed, but thereafter more conserved, again reflecting the probable greater lability of cranial evolution due to lower constraints and greater specificity to adaptation. The pelvic shifts identified likely correspond to major changes in locomotion and feeding, with that at Dinosauromorpha corresponding with the development of cursorial bipedality, that in Ornithischia reflecting the development of an opisthopubic morphology in connection with herbivory, and that in Sauropodomorpha potentially reflecting the evolution of herbivory and graviportal and quadrupedality in the clade (Sander et al., 2011; McPhee et al., 2018). A different pattern is detected for Pseudosuchia, however, with changes in the pelvis low at the base of the clade, but significant upshifts are detected at the base of major clades. This probably reflects diversifications into different ecomorphologies (e.g. heavily armoured aetosaurs, bipedal terrestrial carnivores, aquatic carnivores) in a context of relatively low overall pelvic disparity for the group.

Removal of allometric shape information for the cranium had very little effect on the results, but the additional downshift detected around the base of Crocodylomorpha may reflect a connection between size and longirostry in the clade (i.e. with smaller taxa tending to have shorter rostra); other studies have demonstrated heterochronic processes at play in skull shape in extant taxa (e.g. Morris et al., 2019; Sookias, 2020). For the pelvis, removal of allometric information led to the upshift at Dinosauromorpha failing to be detected; given that morphological radiation in Dinosauria was intimately associated with change (usually increases) in body size (Irmis, 2010; Sookias et al., 2012), removal of allometric data may actually mask relevant signal. In contrast, in Pseudosuchia, the removal of allometric change resulted in detection of an additional rate downshift around the base of Crocodylomorpha; this possibly reflects the close connection between reducing body size and changes towards a more agile, cursorially-adapted pelvis (with very extended pubis and relatively shortened ischium) in early terrestrial crocodylomorphs.

Clade-Specific Rates

When individual *a priori* identified clades were compared with the rest of the tree in terms of evolutionary rates and changes of evolutionary rates, there were mostly no significant differences (and indeed none at all at $p = 0.01$). This may indicate that testing *a priori* defined clades is not the optimal way of identifying shifts in evolutionary rate and change of rate, and thus demonstrates the utility of an automated approach as implemented by the *search.shift* function in *RRPhylo*. It does, however, also demonstrate that the differences in rate and rate of change

seen between groups in the sample at hand are relatively subtle, because if there were dramatic major changes in particular lineages these would be likely to be detected even using a manual approach. The only significant ($p = 0.05$)—and by far the majority of non-significant—differences in rate between *a priori* defined clades and the rest of the tree were examples of lower rates in the clade. This is in accordance with the wider pattern seen of decreasing rates through time, and tendency for clades to show significant downshifts following their radiation. Although there was quite some variation, in the majority of cases—including all those that are significant at $p = 0.05$ —the slope of the *a priori* defined subclades was less steep than that of the tree as a whole. This is again consistent with morphological slowdown and stabilization following the origin of major clades, with less change on average within these clades than seen across the broader tree.

Median Rates Through Time, Radiation, and Extinction

The median time-binned evolutionary rates for the entire dataset show a trend of deceleration through time (see above and **Figure 12**), until reaching a minimum in the Toarcian (cranium) and Pliensbachian (pelvis), and subsequently increasing again during the late Middle and Late Jurassic. A local peak of pelvic evolutionary rates during the Ladinian seems to be related to the diversification of locomotory strategies after a first morphospace expansion during the Anisian (Ezcurra and Butler, 2018; Ezcurra et al., 2021a). The result for the pelvis in particular contrasts with previous studies that found very high evolutionary rates for archosauromorphs as a whole and stem-archosaurs during the Early (as opposed to Middle) Triassic based on discrete characters of the entire skeleton (Ezcurra and Butler, 2018; Ezcurra et al., 2021a). These differences of results may be, at least in part, related to the interpolation method used here and the absence of any correction for ghost lineages in the previous studies. They may also relate to the different means used of capturing morphology, with overall shape perhaps diversifying subsequently to discrete characters—i.e., major ecomorphological diversification being subsequent to phylogenetic diversification. This would be congruent with previous work indicating that diversification is associated with relaxed diversity bounds (e.g. due to continental colonization or post-extinction free niche space) rather than necessarily ecomorphological diversification (e.g. Alhajeri et al., 2016; Cantalapiedra et al., 2017). Furthermore, the continued ecological importance of therapsids during the Early Triassic may have limited scope for ecological, as opposed to phylogenetic, diversification. However, the interpolation method and shape of the archosauromorph phylogenetic tree may also have affected the results: Ezcurra and Butler (2018) calculated the phylogenetic diversity of early archosauromorphs and found that the Induan shows a drop in diversity, and cladogenetic events are concentrated in the late Permian, Olenekian and Middle Triassic. Our interpolation method probably concentrated inferred morphologies in the latter time bins and resulted in low Early Triassic rates driven by the lower number of branches that occur in the Induan. Beyond that, the general pattern of deceleration of rates during the Triassic matches the results recovered by the previously mentioned earlier

studies focused on archosauromorphs (Ezcurra and Butler, 2018; Ezcurra et al., 2021a) and also a similar analysis focused on ichthyosaurs (Moon and Stubbs, 2020). By contrast, the evolutionary rates of Triassic non-mammalian mammaliomorphs increase rather constantly during this period (Close et al., 2015).

The stabilization (cranium) or increase (pelvis) of evolutionary rates since the Toarcian is likely related to the mass extinction event and the diversification of the group as a result of the occupation of empty niches (Benton, 1983; Brusatte et al., 2008a; Brusatte et al., 2008b; Irmis, 2010). A similar pattern of high evolutionary rates and subsequent deceleration have been found in mammaliomorphs (Close et al., 2015), whereas rather constant rates have been found for lepidosaurs in the Early Jurassic (Simões et al., 2020). The increase of evolutionary rates—which is stronger for the pelvis—recovered here for archosauromorphs during the Middle and Late Jurassic partially matches the results found for lepidosaurs, but the latter show a conspicuous deceleration in the Late Jurassic (Simões et al., 2020). By contrast, mammaliomorphs depict a continuous decrease of rates during the Middle and Late Jurassic (Close et al., 2015). Finally, ichthyosaurs show a gradual and slight deceleration of rates during the Jurassic (Moon and Stubbs, 2020). As a result, the Middle and Late Jurassic represent times of adaptive radiation in archosauromorphs, mammaliomorphs, and lepidosaurs, but with each clade displaying a differently-timed peak of evolutionary rates during this period. Thus, the acceleration in morphological evolution present in these groups were probably driven by intrinsic conditions of each clade and/or biological interactions with other clades, not by general environmental factors.

Evolutionary Rates and Wider Evolutionary Processes

Overall, our results shed further light on the wider process of evolutionary diversification. The observed pattern of change slowing through time and being localized around the base of major clades is concordant with previous quantitative work on other clades (Ruta et al., 2006; Harmon et al., 2010; Puttick, 2018) and corresponds broadly to Simpson (1944, 1953) conceptions of adaptive radiations and numerous previous observations of the fossil record (Foote, 1994; Wagner, 1997; Hughes et al., 2013). As explored previously (Harmon et al., 2010), this pattern may not be the result of a strict “early burst” process of declining rates along lineages (as implied by Simpson’s conception), but rather the result of early movement into selective optima and stabilizing selection thereafter (multiple optima under an Ornstein–Uhlenbeck model). This latter pattern can be broadly considered as an “early burst” process, with declining rates at more deeply nested nodes (Puttick, 2018). Under this model, younger clades tend to show higher rates of evolution because of directional selection or selective release, with this effect “cancelled out” by stabilising selection over longer time scales (Gingerich, 1983; Gingerich, 2001; Lynch, 1990; Stanley, 1995; Hendry and Kinnison, 1999; Kinnison and Hendry, 2001; Roopnarine, 2003; Estes and Arnold, 2007). This concept corresponds to the idea of “punctuated equilibrium,” with periods of strong directional selection

punctuating stabilising selection (Eldredge and Gould, 1972; Gould, 2002; Butler and King, 2004; Estes and Arnold, 2007).

Such processes would possibly be more concordant with the localization seen of downshifts in rates at the base of clades entering new ecomorphological niches (e.g. Ceratopsia within Ornithischia), rather than at the very base of the archosauromorph and archosaur radiations, and with the continued rate variation seen within clades. It would also be concordant with the relatively high rates seen in stem-archosaur taxa, which have a relatively short duration because the group went extinct close to or during the Triassic-Jurassic mass extinction. A conclusive distinction between a “true” early burst (i.e. declining rates), restriction around optima, and multiple Brownian regimes would require further investigation. What is, however, likely—given the apparent bursts of evolution at the base of various clades—is that models with multiple optima would fit the data better than those with single rates/optima, agreeing with previous suggestions that strict “early burst” models for very large radiations may not fit the data because repeated bursts of evolution within radiations are common (Puttick, 2018). However, the outcome of the rate analysis depends on the tree topology and the method of time calibration. The ‘equal’ calibration approach employed here to fix the age of the origin of Archosauromorpha (following Ezcurra et al., 2014) represents just one possible calibration approach. Using other calibration methods (see Bapst, 2013; Bapst, 2014) may change the time of this early peak of rates (resulting in older peaks), but will not affect the overall pattern of “early-burst-like” process found by our analyses and its general congruence with higher levels of morphological disparity. The differences seen between the cranium and pelvis also elucidate further the specifics of the process of adaptive radiation, with differing patterns of evolution in different anatomical regions. Some structures (e.g. the skull) are probably more labile than others (e.g. the pelvis), possibly due to lower morphofunctional constraints, with more constrained structures characterizing the “Bauplan” of a group (Blomberg and Garland, 2002; Valentine, 2004). Thus, different patterns of change through time may be expected when different traits and regions are analysed, possibly accounting for the detection of “true” early burst signals in some clades but not in others (see Harmon et al., 2010).

Broader Macroevolutionary Implications

Taken together, the results of the current study lend further support to the idea of a non-competitive replacement of stem by crown-archosaurs, and call into question the level of applicability of the idea of “peak disparity.” Stem-archosaurs were previously demonstrated to show relatively high cranial disparity (Foth et al., 2016a), with crown taxa only expanding fully in disparity following the extinction of many stem taxa. This is confirmed here for the cranium, and also appears to apply to the pelvis, again indicating that crown taxa expanded due to ecological release rather than outcompetition of stem forms. This is further supported by comparing the rates of evolution between stem and crown taxa, with in general very weak evidence for consistent rate differences between the stem and the crown. Indeed, stem taxa show slightly higher rates than crown taxa (significant only

for a few single PC axes—see *Results*), although this may be confounded by the longer period of morphological stasis seen after the development of major crown lineages. This is congruent with much previous work indicating similar patterns of competitive release rather than outcompetition between archosauromorph groups (Brusatte et al., 2008a; Sookias et al., 2012; Foth et al., 2016a).

The apparent failure of archosauromorphs to reach “peak disparity” during the studied interval is notable because it is relatively long—ca. 60 Myr—(Briggs et al., 1992; Erwin, 2007; Hughes et al., 2013), although similar delayed peaks have been previously observed in pterosaurs (Foth et al., 2012), turtles (Foth and Joyce, 2016; Foth et al., 2017), crocodylomorphs (Stubbs et al., 2021) and some mammalian groups (Jernvall et al., 2000; Wesley-Hunt, 2005). Potentially, the artificial truncation of our dataset at the end of the Jurassic may have prevented peak disparity from having been reached by crown-archosaur clades (Hughes et al., 2013). However, work demonstrating early peaks has tended to be focused on taxonomically smaller clades with a more morphofunctionally constrained morphology (e.g. subclades such as ankylosaurs are used by Hughes et al. (2013) rather than Ornithischia or Dinosauria as a whole), whereas the large scale of the archosauromorph radiation would imply that repeated development of novel and disparate body forms in different subclades prevented peak disparity from being reached. Thus, the Triassic-Jurassic archosauromorph radiation seems not to fit the idea of an early peak of disparity, without a peak being reached within a particular ecomorphotype (corresponding to an “early burst” pattern of evolution *sensu lato*), but this may be due to the development of new ecomorphotypes effectively releasing disparity constraints (e.g. by entering another dietary or habitat niche) before a peak is reached.

The current study also helps to address, at least within Archosauromorpha, the question of whether the disparity of different anatomical regions (in this case cranium and pelvic girdle) tends to be correlated, with different regions showing broadly corresponding disparity but with more pronounced differences at lower phylogenetic levels. The lack of correlation between the cranial and pelvic disparity curves of Ornithischia, Sauropodomorpha and Pterosauria is a result of relatively more stable pelvic disparity values through time than those for the cranial dataset. This further supports the idea (see above) that the pelvis—perhaps due to its more directly mechanically functional role—is less plastic to morphological change. This potentially contrasts with the results found for some other groups, where structures involved in locomotion—e.g. limbs—were found to be more labile than the skull (Vidal-García and Keogh, 2017); this points towards taxon specificity of these conclusions, but limbs may potentially be less constrained than the pelvis. Thus, while at lower phylogenetic scales there is support for a “mosaic” pattern of evolution with differing disparity patterns between different regions (see e.g. Felice and Goswami, 2018), at a broader scale these patterns may tend to converge (as it was the case of a significant correlation between cranium and pelvis in the three disparity metrics). The broad correlation in the changes in the position of the morphospace between the cranial and pelvic data

is consistent with a coupled evolutionary model of deceleration of morphospace migration through time for both skeletal partitions.

CONCLUSION

Overall, this study sheds important new light on the early diversification of Archosauromorpha and Archosauria, and has implications for the study of evolutionary diversifications more broadly. We provide evidence for a delayed disparity peak, “early bursts” *sensu lato* of evolutionary change both at larger and smaller phylogenetic scales, and a confirmation of unexpectedly great disparity among stem taxa during this hyperdiverse radiation. All sampled clades of archosauromorphs showed a delayed density-volume disparity peak in both the cranium and pelvis, indicating that disparity was not likely saturated by the end of the studied time span (Late Jurassic), and indeed disparate and unique archosaur clades continue to radiate in the Cretaceous (e.g. ceratopsians, ornithomimosaur, notosuchians). Such delayed disparity peaks may in fact be typical of such large-scale and hyperdiverse radiations, and this area warrants further study. Archosauromorpha shows very high initial rates of cranial and pelvic evolution (Permian-Middle Triassic) followed by lower ones once diversification into more specific niches has occurred (Late Triassic-Jurassic), representing an “early burst” *sensu lato* model. This pattern is accompanied by a decrease of the displacement of the morphospace, with initial evolutionary shifts followed by a period of near-stasis once diversification into niches has occurred. Similar patterns are found within subclades, with very high initial rates as new ecomorphologies develop, followed by relative stability (especially for the pubis). Again, this has wider implications for geological-scale evolutionary radiations more broadly, supporting broad-based evidence of reducing rates through time during such events. Our study also—in contrast to much recent work—finds relatively widespread evidence of a correlation between diversity and disparity, and indicate that—at least in initial parts of adaptive radiations—such patterns may be more commonplace than expected. Correlation, is, however, only widely found using average displacement as a metric, demonstrating the importance of using different diversity metrics to describe the morphospace more comprehensively. Significant correlations of diversity with sum of variances at the largest phylogenetic scales also demonstrate the effect of scale on such results. Our results are congruent with previous results that highlighted an unexpectedly high cranial morphological diversity for stem-archosaurs during the Middle and early Late Triassic, with a similar pattern found for pelvic disparity. The size of the morphospace (see sum of variances) of the pelvic region in stem-archosaurs remained similar to (Early and Middle Triassic) or lower (Late Triassic) than that of pseudosuchians and avemetatarsalians. By contrast, the disparity evidenced in stem-archosaurs *via* the pelvic girdle morphospace (see average nearest neighbor distance) of stem-archosaurs was higher than that of pseudosuchians and avemetatarsalians during most of the Triassic. The latter probably indicates a high diversity in terms of habitat preferences and locomotion styles in stem-archosaurs until their extinction in the latest Triassic. Our study also

indicates greater lability in cranial than pelvic shape during the archosauromorph radiation across all clades, with greater stability of pelvic morphology within clades following development of unique characteristics (e.g. opisthopubic morphology). This potentially demonstrates the greater morphofunctional constraints placed on the pelvis, and the way in which different skeletal partitions can be more or less variable or constrained during evolutionary radiations. Finally, interpolating shape changes along branch lengths allows to estimate, with the proper caution, disparity also for time periods with poor fossil record. The major results are comparable to analyses that include only terminal taxa and hypothetical ancestors, but the interpolation allows for correction of the impact of Lazarus taxa. Using only terminal taxa for disparity analysis, however, can lead to different, flawed outcomes, which are primarily caused by smaller sample sizes and longer time bins. The current study thus demonstrates the utility of usage of interpolated morphologies in more poorly sampled bins in this kind of analysis.

DATA AVAILABILITY STATEMENT

The original contributions presented in the study are included in the article/**Supplementary Material**. Additional supplementary material is stored at <https://zenodo.org> (DOI:10.5281/zenodo.5175797). The (semi-)landmark coordinates (before and after GPA) as well as all PCA results are included in the Morpho file. All cranial and pelvic reconstructions used in this study are available upon request to the corresponding author. In addition, the original R script of Foth et al. (2017) for estimating disparity along phylogenetic trees can be found in the following repository: https://bitbucket.org/eascarrunz/fothetal2017_turtle_disparity.

AUTHOR CONTRIBUTIONS

All authors listed have made a substantial, direct, and intellectual contribution to the work and approved it for publication.

FUNDING

This research was supported by the Swiss National Science Foundation (PZ00P2_174040 to CF), the German Science Foundation (FO 1005/2-1 to CF) and the Agencia Nacional de Promoción Científica y Técnica (PICT 2018-01186 to MDE). During completion of the work, RBS was supported by a Research Fellowship from the Alexander von Humboldt Foundation, by a European Research Council Starting Grant (TEMPO: ERC-2015-STG) to Roger Benson (University of Oxford), and by a position as Chargé de Recherches from the Fonds de la Recherche Scientifique (Wallonia).

ACKNOWLEDGMENTS

We thank Richard Butler and Stephen Brusatte for discussions and comments during an initial phase of

this project. We further thank PG and TS for their evaluation of the study. The authors also sincerely thank Silvia Castiglione and Pasquale Raia for their generous assistance with evolutionary rates analysis with *RRphylo*.

REFERENCES

- Abzhanov, A. (2010). Darwin's Galápagos Finches in Modern Biology. *Phil. Trans. R. Soc. B* 365, 1001–1007. doi:10.1098/rstb.2009.0321
- Alhajeri, B. H., Schenk, J. J., and Stepan, S. J. (2016). Ecomorphological Diversification Following continental Colonization in Muroid Rodents (Rodentia: Muroidea). *Biol. J. Linn. Soc.* 117, 463–481. doi:10.1111/bij.12695
- Anderson, P. S. L., and Friedman, M. (2012). Using Cladistic Characters to Predict Functional Variety: Experiments Using Early Gnathostomes. *J. Vertebr. Paleontol.* 32, 1254–1270. doi:10.1080/02724634.2012.694386
- Andres, B., Clark, J., and Xu, X. (2014). The Earliest Pterodactyloid and the Origin of the Group. *Curr. Biol.* 24, 1011–1016. doi:10.1016/j.cub.2014.03.030
- Bapst, D. W. (2013). A Stochastic Rate-Calibrated Method for Time-Scaling Phylogenies of Fossil Taxa. *Methods Ecol. Evol.* 4, 724–733. doi:10.1111/2041-210x.12081
- Bapst, D. W. (2014). Assessing the Effect of Time-Scaling Methods on Phylogeny-Based Analyses in the Fossil Record. *Paleobiology* 40, 331–351. doi:10.1666/13033
- Bapst, D. W., Bullock, P. C., Melchin, M. J., Sheets, H. D., and Mitchell, C. E. (2012). Graptoloid Diversity and Disparity Became Decoupled during the Ordovician Mass Extinction. *Proc. Natl. Acad. Sci.* 109, 3428–3433. doi:10.1073/pnas.1113870109
- Bapst, D. W. (2012). Paleotree: an R Package for Paleontological and Phylogenetic Analyses of Evolution. *Methods Ecol. Evol.* 3, 803–807. doi:10.1111/j.2041-210x.2012.00223.x
- Baron, M. G. (2019). *Pisanosaurus Mertii* and the Triassic Ornithischian Crisis: Could Phylogeny Offer a Solution? *Hist. Biol.* 31, 967–981. doi:10.1080/08912963.2017.1410705
- Barrett, P. M., Butler, R. J., and Nesbitt, S. J. (2011). The Roles of Herbivory and Omnivory in Early dinosaur Evolution. *Earth Environ. Sci. Trans. R. Soc. Edinb.* 101, 383–396. doi:10.1017/s1755691011020111
- Barrett, P. M. (2014). Paleobiology of Herbivorous Dinosaurs. *Annu. Rev. Earth Planet. Sci.* 42, 207–230. doi:10.1146/annurev-earth-042711-105515
- Barrett, P., and Rayfield, E. (2006). Ecological and Evolutionary Implications of dinosaur Feeding Behaviour. *Trends Ecol. Evol.* 21, 217–224. doi:10.1016/j.tree.2006.01.002
- Bartoń, K. (2018). MuMIn: Multi-model Inference. R package version 1.40.4. <http://cran.r-project.org/package=MuMIn>.
- Benson, R. B., Frigot, R. A., Goswami, A., Andres, B., and Butler, R. J. (2014). Competition and Constraint Drove Cope's Rule in the Evolution of Giant Flying Reptiles. *Nat. Commun.* 5, 3567–3568. doi:10.1038/ncomms4567
- Benson, R. B. J., Evans, M., and Druckenmiller, P. S. (2012). High Diversity, Low Disparity and Small Body Size in Plesiosaurs (Reptilia, Sauropterygia) from the Triassic-Jurassic Boundary. *PLoS ONE* 7, e31838. doi:10.1371/journal.pone.0031838
- Benton, M. J. (1983). Dinosaur success in the Triassic: a Noncompetitive Ecological Model. *Q. Rev. Biol.* 58, 29–55. doi:10.1086/413056
- Benton, M. J., Forth, J., and Langer, M. C. (2014). Models for the Rise of the Dinosaurs. *Curr. Biol.* 24, R87–R95. doi:10.1016/j.cub.2013.11.063
- Benton, M. J. (2003). *When Life Nearly Died: The Greatest Mass Extinction of All Time*. London: Thames & Hudson.
- Benton, M. J., and Walker, A. D. (2002). *Erpetosuchus*, a Crocodile-like Basal Archosaur from the Late Triassic of Elgin, Scotland. *Zool. J. Linn. Soc.* 136, 25–47. doi:10.1046/j.1096-3642.2002.00024.x
- Bernhardt, P. (2000). Convergent Evolution and Adaptive Radiation of Beetle-Pollinated Angiosperms. *Plant Syst. Evol.* 222, 293–320. doi:10.1007/978-3-7091-6306-1_16

SUPPLEMENTARY MATERIAL

The Supplementary Material for this article can be found online at: <https://www.frontiersin.org/articles/10.3389/feart.2021.723973/full#supplementary-material>

- Bestwick, J., Unwin, D. M., Butler, R. J., Henderson, D. M., and Purnell, M. A. (2018). Pterosaur Dietary Hypotheses: a Review of Ideas and Approaches. *Biol. Rev.* 93, 2021–2048. doi:10.1111/brv.12431
- Bird Life International (2020). *Species Factsheet: Mellisuga Helenae*. Downloaded from: <http://www.birdlife.org> on August13, 2020.
- Blomberg, S. P., and Garland, T., Jr. (2002). Tempo and Mode in Evolution: Phylogenetic Inertia, Adaptation and Comparative Methods. *J. Evol. Biol.* 15, 899–910. doi:10.1046/j.1420-9101.2002.00472.x
- Bookstein, F. L. (1997). Landmark Methods for Forms without Landmarks: Morphometrics of Group Differences in Outline Shape. *Med. Image Anal.* 1, 225–243. doi:10.1016/s1361-8415(97)85012-8
- Bookstein, F. L. (1991). *Morphometric Tools for Landmark Data*. Cambridge: Cambridge University Press.
- Bookstein, F., Schäfer, K., Prossinger, H., Seidler, H., Fieder, M., Stringer, C., et al. (1999). Comparing Frontal Cranial Profiles in Archaic and modern Homo by Morphometric Analysis. *Anat. Rec.* 257, 217–224. doi:10.1002/(sici)1097-0185(19991215)257:6<217::aid-ar7>3.0.co;2-w
- Briggs, D. E. G., Fortey, R. A., and Wills, M. A. (1992). Morphological Disparity in the Cambrian. *Science* 256, 1670–1673. doi:10.1126/science.256.5064.1670
- Bronzati, M., Montefeltro, F. C., and Langer, M. C. (2015). Diversification Events and the Effects of Mass Extinctions on Crocodyliformes Evolutionary History. *R. Soc. Open Sci.* 2, 140385. doi:10.1098/rsos.140385
- Brusatte, S. L., Benton, M. J., Ruta, M., and Lloyd, G. T. (2008a). Superiority, Competition, and Opportunism in the Evolutionary Radiation of Dinosaurs. *Science* 321, 1485–1488. doi:10.1126/science.1161833
- Brusatte, S. L., Benton, M. J., Ruta, M., and Lloyd, G. T. (2008b). The First 50 Myr of dinosaur Evolution: Macroevolutionary Pattern and Morphological Disparity. *Biol. Lett.* 4, 733–736. doi:10.1098/rsbl.2008.0441
- Brusatte, S. L., Montanari, S., Yi, H.-y., and Norell, M. A. (2011). Phylogenetic Corrections for Morphological Disparity Analysis: New Methodology and Case Studies. *Paleobiology* 37, 1–22. doi:10.1666/09057.1
- Brusatte, S. L., Nesbitt, S. J., Irmis, R. B., Butler, R. J., Benton, M. J., and Norell, M. A. (2010). The Origin and Early Radiation of Dinosaurs. *Earth-Science Rev.* 101, 68–100. doi:10.1016/j.earscirev.2010.04.001
- Butler, M. A., and King, A. A. (2004). Phylogenetic Comparative Analysis: a Modeling Approach for Adaptive Evolution. *The Am. Naturalist* 164, 683–695. doi:10.2307/3473229
- Butler, R. J., Brusatte, S. L., Andres, B., and Benson, R. B. J. (2012). How Do Geological Sampling Biases Affect Studies of Morphological Evolution in Deep Time? A Case Study of Pterosaur (Reptilia: Archosauria) Disparity. *Evolution* 66, 147–162. doi:10.1111/j.1558-5646.2011.01415.x
- Butler, R. J., Brusatte, S. L., Reich, M., Nesbitt, S. J., Schoch, R. R., and Hornung, J. J. (2011). The Sail-Backed Reptile *Ctenosauriscus* from the Latest Early Triassic of Germany and the Timing and Biogeography of the Early Archosaur Radiation. *PLoS One* 6, e25693. doi:10.1371/journal.pone.0025693
- Butler, R. J., Jones, A. S., Buffetaut, E., Mandl, G. W., Scheyer, T. M., and Schultz, O. (2019a). Description and Phylogenetic Placement of a New marine Species of Phytosaur (Archosauriformes: Phytosauria) from the Late Triassic of Austria. *Zool. J. Linn. Soc.* 187, 198–228. doi:10.1093/zoolinnean/zlz014
- Butler, R. J., Sennikov, A. G., Dunne, E. M., Ezcurra, M. D., Hedrick, B. P., Maidment, S. C. R., et al. (2019b). Cranial Anatomy and Taxonomy of the Erythrosuchid Archosauriform 'Vjushkovia Triplicostata' Huene, 1960, from the Early Triassic of European Russia. *R. Soc. Open Sci.* 6, 191289. doi:10.1098/rsos.191289
- Cantalapiedra, J. L., Prado, J. L., Hernández Fernández, M., and Alberdi, M. T. (2017). Decoupled Ecomorphological Evolution and Diversification in Neogene-Quaternary Horses. *Science* 355, 627–630. doi:10.1126/science.aag1772

- Carrano, M. T. (1999). What, if Anything, Is a Cursor? Categories versus Continua for Determining Locomotor Habit in Mammals and Dinosaurs. *J. Zool.* 247, 29–42. doi:10.1111/j.1469-7998.1999.tb00190.x
- Carpenter, K., DiCroce, T., Kinneer, B., and Simon, R. (2013). Pelvis of *Gargoyleosaurus* (Dinosauria: Ankylosauria) and the Origin and Evolution of the Ankylosaur Pelvis. *PLoS One* 8, e79887. doi:10.1371/journal.pone.0079887
- Castiglione, S., Serio, C., Tamagnini, D., Melchionna, M., Mondanaro, A., Di Febraro, M., et al. (2019). A New, Fast Method to Search for Morphological Convergence with Shape Data. *PLoS One* 14, e0226949. doi:10.1371/journal.pone.0226949
- Castiglione, S., Tesone, G., Piccolo, M., Melchionna, M., Mondanaro, A., Serio, C., et al. (2018). A New Method for Testing Evolutionary Rate Variation and Shifts in Phenotypic Evolution. *Methods Ecol. Evol.* 9, 974–983. doi:10.1111/2041-210x.12954
- Cavin, L., and Forey, P. L. (2007). Using Ghost Lineages to Identify Diversification Events in the Fossil Record. *Biol. Lett.* 3, 201–204. doi:10.1098/rsbl.2006.0602
- Chivers, D. J., and Hladik, C. M. (1980). Morphology of the Gastrointestinal Tract in Primates: Comparisons with Other Mammals in Relation to Diet. *J. Morphol.* 166, 337–386. doi:10.1002/jmor.1051660306
- Clarke, M., Thomas, G. H., and Freckleton, R. P. (2017). Trait Evolution in Adaptive Radiations: Modeling and Measuring Interspecific Competition on Phylogenies. *Am. Naturalist* 189, 121–137. doi:10.1086/689819
- Close, R. A., Friedman, M., Lloyd, G. T., and Benson, R. B. (2015). Evidence for a Mid-Jurassic Adaptive Radiation in Mammals. *Curr. Biol.* 25, 2137–2142. doi:10.1016/j.cub.2015.06.047
- Cooney, C. R., Bright, J. A., Capp, E. J. R., Chira, A. M., Hughes, E. C., Moody, C. J. A., et al. (2017). Mega-evolutionary Dynamics of the Adaptive Radiation of Birds. *Nature* 542, 344–347. doi:10.1038/nature21074
- de Vita, J. (1979). Niche Separation and the Broken-Stick Model. *Am. Naturalist* 114, 171–178. doi:10.1086/283466
- Desojo, J. B., Fiorelli, L. E., Ezcurra, M. D., Martinelli, A. G., Ramezani, J., Da Rosa, Á. A. S., et al. (2020). The Late Triassic Ischigualasto Formation at Cerro Las Lajas (La Rioja, Argentina): Fossil Tetrapods, High-Resolution Chronostratigraphy, and Faunal Correlations. *Sci. Rep.* 10, 12782. doi:10.1038/s41598-020-67854-1
- Desojo, J. B., Heckert, A. B., Martz, J. W., Parker, W. G., Schoch, R. R., Small, B. J., et al. (2013). Aetosauria: a Clade of Armoured Pseudosuchians from the Upper Triassic continental Beds. *Geol. Soc. Lond. Spec. Publications* 379, 203–239. doi:10.1144/sp379.17
- Dzik, J., and Sulej, T. (2016). An Early Late Triassic Long-Necked Reptile with a Bony Pectoral Shield and Gracile Appendages. *Acta Palaeontol. Pol.* 61, 805–823.
- Eldredge, N., and Gould, S. J. (1972). “Punctuated Equilibria: an Alternative to Phyletic Gradualism,” in *Models in Paleobiology*. Editor T. J. M. Schopf (San Francisco: Freeman, Cooper & Co), 82–115.
- Erwin, D. H. (2007). Disparity: Morphological Pattern and Developmental Context. *Palaeontology* 50, 57–73. doi:10.1111/j.1475-4983.2006.00614.x
- Estes, S., and Arnold, S. J. (2007). Resolving the Paradox of Stasis: Models with Stabilizing Selection Explain Evolutionary Divergence on All Timescales. *Am. Naturalist* 169, 227–244. doi:10.1086/510633
- Ezcurra, M. D., and Butler, R. J. (2018). The Rise of the Ruling Reptiles and Ecosystem Recovery from the Permo-Triassic Mass Extinction. *Proc. R. Soc. B.* 285, 20180361. doi:10.1098/rspb.2018.0361
- Ezcurra, M. D., Jones, A. S., Gentil, A. R., and Butler, R. J. (2021a). “Early Archosauromorphs: The Crocodile and Dinosaur Precursors,” in *Encyclopedia of Geology*. Editors D. Alderton and S. A. Elias. 2nd edition (United Kingdom: Academic Press), Vol. 4, 175–185. doi:10.1016/b978-0-12-409548-9.12439-x
- Ezcurra, M. D., Montefeltro, F. C., and Butler, R. J. (2016). The Early Evolution of Rhynchosaurs. *Front. Ecol. Evol.* 3, 1–23. doi:10.3389/fevo.2015.00142
- Ezcurra, M. D., Montefeltro, F. C., Pinheiro, F. L., Trotteyn, M. J., Gentil, A. R., Lehmann, O. E. R., et al. (2021b). The Stem-Archosaur Evolutionary Radiation in South America. *J. South Am. Earth Sci.* 105, 102935. doi:10.1016/j.jsames.2020.102935
- Ezcurra, M. D., Nesbitt, S. J., Bronzati, M., Dalla Vecchia, F. M., Agnolin, F. L., Benson, R. B. J., et al. (2020). Enigmatic dinosaur Precursors Bridge the gap to the Origin of Pterosauria. *Nature* 588, 445–449. doi:10.1038/s41586-020-3011-4
- Ezcurra, M. D., Scheyer, T. M., and Butler, R. J. (2014). The Origin and Early Evolution of Sauria: Reassessing the Permian Saurian Fossil Record and the Timing of the Crocodile-Lizard Divergence. *PLoS One* 9, e89165. doi:10.1371/journal.pone.0089165
- Ezcurra, M. D. (2016). The Phylogenetic Relationships of Basal Archosauromorphs, with an Emphasis on the Systematics of Proterosuchian Archosauriforms. *PeerJ* 4, e1778. doi:10.7717/peerj.1778
- Felice, R. N., and Goswami, A. (2018). Developmental Origins of Mosaic Evolution in the Avian Cranium. *Proc. Natl. Acad. Sci. U.S.A.* 115, 555–560. doi:10.1073/pnas.1716437115
- Foote, M. (1991). Morphological and Taxonomic Diversity in a Clade’s History: the Blastoid Record and Stochastic Simulations. *Contrib. Mus. Paleontol.* 28, 101–140.
- Foote, M. (1994). Morphological Disparity in Ordovician-Devonian Crinoids and the Early Saturation of Morphological Space. *Paleobiology* 20, 320–344. doi:10.1017/s009483730001280x
- Fortey, R. A., Briggs, D. E. G., and Wills, M. A. (1996). The Cambrian Evolutionary ‘explosion’: Decoupling Cladogenesis from Morphological Disparity. *Biol. J. Linn. Soc.* 57, 13–33. doi:10.1111/j.1095-8312.1996.tb01693.x
- Foth, C., Ascarrunz, E., and Joyce, W. G. (2017). Still Slow, but Even Steadier: an Update on the Evolution of Turtle Cranial Disparity Interpolating Shapes along Branches. *R. Soc. Open Sci.* 4, 170899. doi:10.1098/rsos.170899
- Foth, C., Brusatte, S. L., and Butler, R. J. (2012). Do different Disparity Proxies Converge on a Common Signal? Insights from the Cranial Morphometrics and Evolutionary History of Pterosauria (Diapsida: Archosauria). *J. Evol. Biol.* 25, 904–915. doi:10.1111/j.1420-9101.2012.02479.x
- Foth, C., Ezcurra, M. D., Sookias, R. B., Brusatte, S. L., and Butler, R. J. (2016a). Unappreciated Diversification of Stem Archosaurs during the Middle Triassic Predated the Dominance of Dinosaurs. *BMC Evol. Biol.* 16, 188. doi:10.1186/s12862-016-0761-6
- Foth, C., Hedrick, B. P., and Ezcurra, M. D. (2016b). Cranial Ontogenetic Variation in Early Saurischians and the Role of Heterochrony in the Diversification of Predatory Dinosaurs. *PeerJ* 4, e1589. doi:10.7717/peerj.1589
- Foth, C., and Joyce, W. G. (2016). Slow and Steady: the Evolution of Cranial Disparity in Fossil and Recent Turtles. *Proc. R. Soc. B.* 283, 20161881. doi:10.1098/rspb.2016.1881
- Foth, C., and Rauhut, O. W. M. (2013). The Good, the Bad, and the Ugly: the Influence of Skull Reconstructions and Intraspecific Variability in Studies of Cranial Morphometrics in Theropods and Basal Saurischians. *PLoS One* 8, e72007. doi:10.1371/journal.pone.0072007
- Friedman, M. (2009). Ecomorphological Selectivity Among marine Teleost Fishes during the End-Cretaceous Extinction. *Proc. Natl. Acad. Sci.* 106, 5218–5223. doi:10.1073/pnas.0808468106
- Gingerich, P. D. (2001). “Rates of Evolution on the Time Scale of the Evolutionary Process,” in *Microevolution Rate, Pattern, Process*. Editors A. P. Hendry and M. T. Kinnison (Dordrecht: Springer), 127–144. doi:10.1007/978-94-010-0585-2_9
- Gingerich, P. D. (1983). Rates of Evolution: Effects of Time and Temporal Scaling. *Science* 222, 159–161. doi:10.1126/science.222.4620.159
- Godoy, P. L., Benson, R. B. J., Bronzati, M., and Butler, R. J. (2019). The Multi-Peak Adaptive Landscape of Crocodylomorph Body Size Evolution. *BMC Evol. Biol.* 19, 167. doi:10.1186/s12862-019-1466-4
- Goolsby, E. W., Bruggeman, J., and Ané, C. (2017). Rphylopars: Fast Multivariate Phylogenetic Comparative Methods for Missing Data and Within-species Variation. *Methods Ecol. Evol.* 8, 22–27. doi:10.1111/2041-210x.12612
- Gould, S. J. (2002). *The Structure of Evolutionary Theory*. Cambridge MA: Harvard University Press.
- Gower, D. J. (2003). Osteology of the Early Archosaurian Reptile *Erythrosuchus africanus* Broom. *Ann. South. Afr. Mus.* 110, 1–84.
- Grenard, S. (1991). *Handbook of Alligators and Crocodiles*. Malabar: Krieger Publishing.
- Guillermo, T., and Cooper, N. (2018). Time for a Rethink: Time Sub-sampling Methods in Disparity-through-time Analyses. *Palaeontology* 61, 481–493. doi:10.1111/pala.12364
- Guillermo, T. (2018). *disPRity*: a Modular R Package for Measuring Disparity. *Methods Ecol. Evol.* 9, 1755–1763. doi:10.1111/2041-210x.13022
- Guillermo, T., Puttick, M. N., Marcy, A. E., and Weisbecker, V. (2020). Shifting Spaces: Which Disparity or Dissimilarity Measurement Best Summarize

- Occupancy in Multidimensional Spaces? *Ecol. Evol.* 10, 7261–7275. doi:10.1002/ece3.6452
- Gunz, P., Mitteroecker, P., and Bookstein, F. L. (2004). “Semilandmarks in Three Dimensions,” in *Modern Morphometrics in Physical Anthropology*. Editor D. E. Slice (New York: Kluwer Academic/Plenum Publishers), 73–98.
- Hammer, O., and Harper, D. A. T. (2006). *Paleontological Data Analysis*. Malden: Blackwell Publishing.
- Hammer, O., Harper, D. A. T., and Ryan, P. D. (2001). PAST: Paleontological Statistics Software Package for Education and Data Analysis. *Palaeontol. Electron.* 4, 1–9.
- Harmon, L. J., Losos, J. B., Jonathan Davies, T., Gillespie, R. G., Gittleman, J. L., Bryan Jennings, W., et al. (2010). Early Bursts of Body Size and Shape Evolution Are Rare in Comparative Data. *Evolution* 64, 2385–2396. doi:10.1111/j.1558-5646.2010.01025.x
- Heimhofer, U., Hochuli, P. A., Burla, S., Dinis, J. M. L., and Weissert, H. (2005). Timing of Early Cretaceous Angiosperm Diversification and Possible Links to Major Paleoenvironmental Change. *Geol.* 33, 141–144. doi:10.1130/g21053.1
- Henderson, D. M. (2002). The Eyes Have it: the Sizes, Shapes, and Orientations of Theropod Orbits as Indicators of Skull Strength and Bite Force. *J. Vertebr. Paleontol.* 22, 766–778.
- Hendry, A. P., and Kinnison, M. T. (1999). Perspective: the Pace of Modern Life: Measuring Rates of Contemporary Microevolution. *Evolution* 53, 1637–1653. doi:10.1111/j.1558-5646.1999.tb04550.x
- Hernández-Hernández, T. (2019). Evolutionary Rates and Adaptive Radiations. *Biol. Philos.* 34, 1–33. doi:10.1007/s10539-019-9694-y
- Higham, T. E., and Russell, A. P. (2010). Divergence in Locomotor Performance, Ecology, and Morphology between Two Sympatric Sister Species of Desert-Dwelling Gecko. *Biol. J. Linn. Soc.* 101, 860–869. doi:10.1111/j.1095-8312.2010.01539.x
- Hughes, M., Gerber, S., and Wills, M. A. (2013). Clades Reach Highest Morphological Disparity Early in Their Evolution. *Proc. Natl. Acad. Sci. USA* 110, 13875–13879. doi:10.1073/pnas.1302642110
- Hunt, G. (2006). Fitting and Comparing Models of Phyletic Evolution: Random Walks and beyond. *Paleobiology* 32, 578–601. doi:10.1666/05070.1
- Hutchinson, J. R. (2006). The Evolution of Locomotion in Archosaurs. *Comptes Rendus Palevol.* 5, 519–530. doi:10.1016/j.crpv.2005.09.002
- Hutchinson, J. R. (2001). The Evolution of Pelvic Osteology and Soft Tissues on the Line to Extant Birds (Neornithes). *Zool. J. Linn. Soc.* 131, 123–168. doi:10.1111/j.1096-3642.2001.tb01313.x
- Irmis, R. B. (2010). Evaluating Hypotheses for the Early Diversification of Dinosaurs. *Earth Environ. Sci. Trans. R. Soc. Edinb.* 101, 397–426. doi:10.1017/s1755691011020068
- Jackson, D. A. (1993). Stopping Rules in Principal Components Analysis: a Comparison of Heuristical and Statistical Approaches. *Ecology* 74, 2204–2214. doi:10.2307/1939574
- Jaquier, V. P., Fraser, N. C., Furrer, H., and Scheyer, T. M. (2017). Osteology of a New Specimen of *Macrocnemus* Aff. *M. Fuyuanensis* (Archosauromorpha, Protosauropoda) from the Middle Triassic of Europe: Potential Implications for Species Recognition and Paleogeography of Tanystropheid Protosauropods. *Front. Earth Sci.* 5, 91. doi:10.3389/feart.2017.00091
- Jernvall, J., Hunter, J. P., and Fortelius, M. (2000). “Trends in the Evolution of Molar crown Types in Ungulate Mammals: Evidence from the Northern Hemisphere,” in *Development, Function and Evolution of Teeth*. Editors M. F. Teaford, M. M. Smith, and M. W. J. Ferguson (Cambridge: Cambridge University Press), 269–281. doi:10.1017/cbo9780511542626.019
- Jetz, W., Thomas, G. H., Joy, J. B., Hartmann, K., and Mooers, A. O. (2012). The Global Diversity of Birds in Space and Time. *Nature* 491, 444–448. doi:10.1038/nature11631
- Jonsson, K. A., Fabre, P.-H., Fritz, S. A., Etienne, R. S., Ricklefs, R. E., Jorgensen, T. B., et al. (2012). Ecological and Evolutionary Determinants for the Adaptive Radiation of the Madagascan Vangas. *Proc. Natl. Acad. Sci.* 109, 6620–6625. doi:10.1073/pnas.1115835109
- Jorgensen, M. E., and Reilly, S. M. (2013). Phylogenetic Patterns of Skeletal Morphometrics and Pelvic Traits in Relation to Locomotor Mode in Frogs. *J. Evol. Biol.* 26, 929–943. doi:10.1111/jeb.12128
- Kinnison, M. T., and Hendry, A. P. (2001). “The Pace of Modern Life II: from Rates of Contemporary Microevolution to Pattern and Process,” in *Microevolution Rate, Pattern, Process*. Editors A. P. Hendry and M. T. Kinnison (Dordrecht: Springer), 145–164. doi:10.1007/978-94-010-0585-2_10
- Kley, N. J., Sertich, J. J. W., Turner, A. H., Krause, D. W., O’Connor, P. M., and Georgi, J. A. (2010). Craniofacial Morphology of *Simosuchus clarki* (Crocodyliformes: Notosuchia) from the Late Cretaceous of Madagascar. *J. Vertebr. Paleontol.* 30, 13–98. doi:10.1080/02724634.2010.532674
- Klingenberg, C. P. (2011). *MorphoJ*: an Integrated Software Package for Geometric Morphometrics. *Mol. Ecol. Resour.* 11, 353–357. doi:10.1111/j.1755-0998.2010.02924.x
- Li, C., Wu, X.-c., Cheng, Y.-n., Sato, T., and Wang, L. (2006). An Unusual Archosauroid from the marine Triassic of China. *Naturwissenschaften* 93, 200–206. doi:10.1007/s00114-006-0097-y
- Lü, J., Azuma, Y., Dong, Z., Barsbold, R., Kobayashi, Y., and Lee, Y.-N. (2009). New Material of Dsungaripterid Pterosaurs (Pterosauria: Pterodactyloidea) from Western Mongolia and its Palaeoecological Implications. *Geol. Mag.* 146, 690–700. doi:10.1017/s0016756809006414
- Lynch, M. (1990). The Rate of Morphological Evolution in Mammals from the Standpoint of the Neutral Expectation. *Am. Naturalist* 136, 727–741. doi:10.1086/285128
- Madsen, O., Scally, M., Douady, C. J., Kao, D. J., DeBry, R. W., Adkins, R., et al. (2001). Parallel Adaptive Radiations in Two Major Clades of Placental Mammals. *Nature* 409, 610–614. doi:10.1038/35054544
- Maidment, S. C. R., and Barrett, P. M. (2012). Does Morphological Convergence Imply Functional Similarity? A Test Using the Evolution of Quadrupedalism in Ornithischian Dinosaurs. *Proc. R. Soc. B.* 279, 3765–3771. doi:10.1098/rspb.2012.1040
- Mannion, P. D., Benson, R. B. J., Carrano, M. T., Tennant, J. P., Judd, J., and Butler, R. J. (2015). Climate Constrains the Evolutionary History and Biodiversity of Crocodylians. *Nat. Commun.* 6, 8438. doi:10.1038/ncomms9438
- Martínez, R. N. (2009). *Adeopapposaurus mognai*, gen. et sp. nov. (Dinosauria: Sauropodomorpha), with comments on adaptations of basal Sauropodomorpha. *J. Vertebr. Paleontol.* 29, 142–164. doi:10.1671/039.029.0102
- Marx, F. G., and Fordyce, R. E. (2015). Baleen Boom and Bust: a Synthesis of Mysticete Phylogeny, Diversity and Disparity. *R. Soc. Open Sci.* 2, 140434. doi:10.1098/rsos.140434
- McPhee, B. W., Benson, R. B. J., Botha-Brink, J., Bordy, E. M., and Choiniere, J. N. (2018). A Giant dinosaur from the Earliest Jurassic of South Africa and the Transition to Quadrupedality in Early Sauropodomorphs. *Curr. Biol.* 28, 3143–e7. doi:10.1016/j.cub.2018.07.063
- Michaud, M., Veron, G., Peigné, S., Blin, A., and Fabre, A.-C. (2018). Are Phenotypic Disparity and Rate of Morphological Evolution Correlated with Ecological Diversity in Carnivora? *Biol. J. Linn. Soc.* 124, 294–307. doi:10.1093/biolinnean/bly047
- Moon, B. C., and Stubbs, T. L. (2020). Early High Rates and Disparity in the Evolution of Ichthyosaurs. *Commun. Biol.* 3, 68–8. doi:10.1038/s42003-020-0779-6
- Morris, Z. S., Vliet, K. A., Abzhanov, A., and Pierce, S. E. (2019). Heterochronic Shifts and Conserved Embryonic Shape Underlie Crocodylian Craniofacial Disparity and Convergence. *Proc. R. Soc. B.* 286, 20182389. doi:10.1098/rspb.2018.2389
- Navalón, G., Bright, J. A., Marugán-Lobón, J., and Rayfield, E. J. (2018). The Evolutionary Relationship Among Beak Shape, Mechanical Advantage, and Feeding Ecology in Modern Birds*. *Evolution* 73, 422–435. doi:10.1111/evo.13655
- Nesbitt, S. J., Brusatte, S. L., Desojo, J. B., Liparini, A., De França, M. A. G., Weinbaum, J. C., et al. (2013). *Rauisuchia*. *Geol. Soc. Lond. Spec. Publications* 379, 241–274. doi:10.1144/sp379.1
- Nesbitt, S. J., Flynn, J. J., Pritchard, A. C., Parrish, J. M., Ranivoharimanana, L., and Wyss, A. R. (2015). Postcranial Osteology of *Azendohsaurus madagaskarensis* (? Middle to Upper Triassic, Isalo Group, Madagascar) and its Systematic Position Among Stem Archosaur Reptiles. *Bull. Am. Mus. Nat. Hist.* 398, 1–126. doi:10.1206/amnb-899-00-1-126.1
- Pinheiro, J., Bates, D., DebRoy, S., and Sarkar, D. R. Core Team (2018). *Nlme: Linear and Nonlinear Mixed Effects Models*. R package version 3.1-137, <https://CRAN.R-project.org/package=nlme>.
- Pinto, G., Mahler, D. L., Harmon, L. J., and Losos, J. B. (2008). Testing the Island Effect in Adaptive Radiation: Rates and Patterns of Morphological

- Diversification in Caribbean and mainland *Anolis* Lizards. *Proc. R. Soc. B.* 275, 2749–2757. doi:10.1098/rspb.2008.0686
- Prentice, K. C., Ruta, M., and Benton, M. J. (2011). Evolution of Morphological Disparity in Pterosaurs. *J. Syst. Palaeontology* 9, 337–353. doi:10.1080/14772019.2011.565081
- Puttick, M. N., Guillaume, T., and Wills, M. A. (2020). The Complex Effects of Mass Extinctions on Morphological Disparity. *Evolution* 74, 2207–2220. doi:10.1111/evo.14078
- Puttick, M. N. (2018). Mixed Evidence for Early Bursts of Morphological Evolution in Extant Clades. *J. Evol. Biol.* 31, 502–515. doi:10.1111/jeb.13236
- R Development Core Team (2011). *R: A Language and Environment for Statistical Computing*. Available at: <http://www.r-project.org>.
- Rauhut, O. W. M. (2014). New Observations on the Skull of *Archaeopteryx*. *Paläontol. Z.* 88, 211–221. doi:10.1007/s12542-013-0186-0
- Rauhut, O. W. M., and Foth, C. (2020). “The Origin of Birds: Current Consensus, Controversy, and the Occurrence of Feathers,” in *The Evolution of Feathers*. Editors C. Foth and O. W. M. Rauhut (Cham: Springer Nature), 27–45. doi:10.1007/978-3-030-27223-4_3
- Raup, D. M., and Sepkoski, J. J. (1982). Mass Extinctions in the marine Fossil Record. *Science* 215, 1501–1503. doi:10.1126/science.215.4539.1501
- Renesto, S., Dalla Vecchia, F. M., and Peters, D. S. (2002). Morphological Evidence for Bipedalism in the Late Triassic Prolacertiform Reptile *Langobardisaurus*. *Senckenbergiana lethaea* 82, 95–106. doi:10.1007/bf03043775
- Renesto, S., and Saller, F. (2018). Evidences for a Semi-aquatic Life Style in the Triassic Diapsid Reptile *Tanystropheus*. *Riv. Ital. di Paleontol. e Stratigr.* 124, 23–34.
- Rohlf, F. J., and Slice, D. (1990). Extensions of the Procrustes Method for the Optimal Superimposition of Landmarks. *Syst. Zoology* 39, 40–59. doi:10.2307/2992207
- Rohlf, F. J. (2005). *tpsDig, Digitize Landmarks and Outlines*. version 2.05.
- Roopnarine, P. D. (2003). Analysis of Rates of Morphologic Evolution. *Annu. Rev. Ecol. Syst.* 34, 605–632. doi:10.1146/annurev.ecolsys.34.011802.132407
- Ruta, M., Botha-Brink, J., Mitchell, S. A., and Benton, M. J. (2013). The Radiation of Cynodonts and the Ground Plan of Mammalian Morphological Diversity. *Proc. R. Soc. B.* 280, 20131865. doi:10.1098/rspb.2013.1865
- Ruta, M., Wagner, P. J., and Coates, M. I. (2006). Evolutionary Patterns in Early Tetrapods. I. Rapid Initial Diversification Followed by Decrease in Rates of Character Change. *Proc. R. Soc. B.* 273, 2107–2111. doi:10.1098/rspb.2006.3577
- Sander, P. M., Christian, A., Clauss, M., Fechner, R., Gee, C. T., Griebeler, E.-M., et al. (2011). Biology of the Sauropod Dinosaurs: the Evolution of Gigantism. *Biol. Rev.* 86, 117–155. doi:10.1111/j.1469-185x.2010.00137.x
- Schachner, E. R., Manning, P. L., and Dodson, P. (2011). Pelvic and Hindlimb Myology of the Basal Archosaur *Poposaurus Gracilis* (Archosauria: Poposauroidae). *J. Morphol.* 272, 1464–1491. doi:10.1002/jmor.10997
- Schluter, D. (2000). *The Ecology of Adaptive Radiation*. Oxford: OUP, 302.
- Schweizer, M., Hertwig, S. T., and Seehausen, O. (2014). Diversity versus Disparity and the Role of Ecological Opportunity in a continental Bird Radiation. *J. Biogeogr.* 41, 1301–1312. doi:10.1111/jbi.12293
- Seehausen, O. (2006). African Cichlid Fish: a Model System in Adaptive Radiation Research. *Proc. Biol. Sci.* 273, 1987–1998. doi:10.1098/rspb.2006.3539
- Sereno, P. C., Martínez, R. N., and Alcober, O. A. (2013). Osteology of *Eoraptor lunensis* (Dinosauria, Sauropodomorpha). *J. Vertebr. Paleontol. Mem.* 12, 83–179. doi:10.1080/02724634.2013.820113
- Sereno, P. C., and Dong, Z. (1992). The Skull of the Basal stegosaur *Huayangosaurus Taibaii* and a Cladistic Diagnosis of Stegosauria. *J. Vertebr. Paleontol.* 12, 318–343. doi:10.1080/02724634.1992.10011463
- Sharov, A. G. (1971). [New Flying Reptiles from the Mesozoic of Kazakhstan and Kirghizia]. *Tr. Paleontol. Inst. Akad. Nauk S.S.R.* 130, 104–113. [in Russian].
- Simões, M., Breitkreuz, L., Alvarado, M., Baca, S., Cooper, J. C., Heins, L., et al. (2016). The Evolving Theory of Evolutionary Radiations. *Trends Ecol. Evol.* 31, 27–34. doi:10.1016/j.tree.2015.10.007
- Simões, T. R., Vernygora, O., Caldwell, M. W., and Pierce, S. E. (2020). Megaevolutionary Dynamics and the Timing of Evolutionary Innovation in Reptiles. *Nat. Commun.* 11, 3322. doi:10.1038/s41467-020-17190-9
- Simpson, G. G. (1953). *Major Features of Evolution*. New York: Columbia Univ. Press.
- Simpson, G. G. (1944). *Tempo and Mode in Evolution*. New York: Columbia Univ. Press.
- Sookias, R. B., Butler, R. J., and Benson, R. B. J. (2012). Rise of Dinosaurs Reveals Major Body-Size Transitions Are Driven by Passive Processes of Trait Evolution. *Proc. R. Soc. B.* 279, 2180–2187. doi:10.1098/rspb.2011.2441
- Sookias, R. B., Dilkes, D., Sobral, G., Smith, R. M. H., Wolvaardt, F. P., Arcucci, A. B., et al. (2020). The Craniomandibular Anatomy of the Early Archosauriform *Euparkeria Capensis* and the Dawn of the Archosaur Skull. *R. Soc. Open Sci.* 7, 200116. doi:10.1098/rsos.200116
- Sookias, R. B. (2020). Exploring the Effects of Character Construction and Choice, Outgroups and Analytical Method on Phylogenetic Inference from Discrete Characters in Extant Crocodylians. *Zool. J. Linn. Soc.* 189, 670–699. doi:10.1093/zoolinnean/zlz015
- Spiekman, S. N. F., and Scheyer, T. M. (2019). A Taxonomic Revision of the Genus *Tanystropheus* (Archosauromorpha, Tanystropheidae). *Palaeontol. Electron.* 22, 1–46. doi:10.26879/1038
- Stanley, S. M. (1995). A Theory of Evolution above the Species Level. *Proc. Natl. Acad. Sci. U S A.* 72, 646–650. doi:10.1073/pnas.72.2.646
- Stubbs, T. L., Pierce, S. E., Elslser, A., Anderson, P. S. L., Rayfield, E. J., and Benton, M. J. (2021). Ecological Opportunity and the Rise and Fall of Crocodylomorph Evolutionary Innovation. *Proc. R. Soc. B.* 288, 20210069. doi:10.1098/rspb.2021.0069
- Stubbs, T. L., Pierce, S. E., Rayfield, E. J., and Anderson, P. S. L. (2013). Morphological and Biomechanical Disparity of Crocodile-Line Archosaurs Following the End-Triassic Extinction. *Proc. R. Soc. B.* 280, 20131940. doi:10.1098/rspb.2013.1940
- Toljagić, O., and Butler, R. J. (2013). Triassic-Jurassic Mass Extinction as Trigger for the Mesozoic Radiation of Crocodylomorphs. *Biol. Lett.* 9, 20130095. doi:10.1098/rsbl.2013.0095
- Tykoski, R. S. (2005). *Anatomy, Ontogeny, and Phylogeny of Coelophysoid Theropods*. Austin: The University of Texas.
- Valentine, J. W. (2004). *On the Origin of Phyla*. Chicago: University of Chicago Press.
- Verde Arregoitia, L. D., Fisher, D. O., and Schweizer, M. (2017). Morphology Captures Diet and Locomotor Types in Rodents. *R. Soc. Open Sci.* 4, 160957. doi:10.1098/rsos.160957
- Vidal-García, M., and Scott Keogh, J. (2017). Phylogenetic Conservatism in Skulls and Evolutionary Lability in Limbs - Morphological Evolution across an Ancient Frog Radiation Is Shaped by Diet, Locomotion and Burrowing. *BMC Evol. Biol.* 17, 165. doi:10.1186/s12862-017-0993-0
- Wagner, P. J. (1997). Patterns of Morphologic Diversification Among the Rostroconchia. *Paleobiology* 23, 115–150. doi:10.1017/s0094837300016675
- Weishampel, D. B., Dodson, P., and Osmólska, H. (2004). *The Dinosauria*. Berkeley: University of California Press.
- Weishampel, D. B., and Norman, D. B. (1989). Vertebrate Herbivory in the Mesozoic; Jaws, Plants, and Evolutionary Metrics. *Geol. Soc. Am. Spec. Pap.* 238, 87–101. doi:10.1130/spe238-p87
- Wellnhofer, P. (1978). *Pterosauria*. Stuttgart, New York: Gustav Fischer Verlag.
- Wesley-Hunt, G. D. (2005). The Morphological Diversification of Carnivores in North America. *Paleobiology* 31, 35–55. doi:10.1666/0094-8373(2005)031<0035:tmddoc>2.0.co;2
- Wilberg, E. W. (2017). Investigating Patterns of Crocodyliform Cranial Disparity through the Mesozoic and Cenozoic. *Zool. J. Linn. Soc.* 181, 189–208. doi:10.1093/zoolinnean/zlw027
- Wills, M. A., Briggs, D. E. G., and Fortey, R. A. (1994). Disparity as an Evolutionary index: a Comparison of Cambrian and Recent Arthropods. *Paleobiology* 20, 93–130. doi:10.1017/s009483730001263x
- Wills, M. A. (2001). “Morphological Disparity: a Primer,” in *Fossils, Phylogeny, and Form: An Analytical Approach*. Editors J. M. Adrain, G. D. Edgecombe, and B. S. Lieberman (Boston: Springer), 55–144. doi:10.1007/978-1-4615-0571-6_4
- Wu, X.-c., Sues, H.-D., and Sun, A. (1995). A Plant-Eating Crocodyliform Reptile from the Cretaceous of China. *Nature* 376, 678–680. doi:10.1038/376678a0
- Zelditch, M. L., Swiderski, D. L., and Sheets, H. D. (2012). *Geometric Morphometrics for Biologists: A Primer*. Amsterdam: Elsevier Academic Press.
- Ósi, A., Young, M. T., Galácz, A., and Rabi, M. (2018). A New Large-Bodied Thalattosuchian Crocodyliform from the Lower Jurassic (Toarcian) of

Hungary, with Further Evidence of the Mosaic Acquisition of marine Adaptations in Metriorhynchoidea. *PeerJ* 6, e4668. doi:10.7717/peerj.4668
Ósi, A. (2015). Feeding-related Characters in Basal Pterosaurs: Implications for Jaw Mechanism, Dental Function and Diet. *Lethaia* 44, 136–152.

Conflict of Interest: The authors declare that the research was conducted in the absence of any commercial or financial relationships that could be construed as a potential conflict of interest.

Publisher's Note: All claims expressed in this article are solely those of the authors and do not necessarily represent those of their affiliated organizations, or those of

the publisher, the editors and the reviewers. Any product that may be evaluated in this article, or claim that may be made by its manufacturer, is not guaranteed or endorsed by the publisher.

Copyright © 2021 Foth, Sookias and Ezcurra. This is an open-access article distributed under the terms of the Creative Commons Attribution License (CC BY). The use, distribution or reproduction in other forums is permitted, provided the original author(s) and the copyright owner(s) are credited and that the original publication in this journal is cited, in accordance with accepted academic practice. No use, distribution or reproduction is permitted which does not comply with these terms.